Quasi-Monte Carlo methods for uncertainty quantification of tumor growth modeled by a parametric semi-linear parabolic reaction-diffusion equation*

Alexander D. Gilbert[†] Frances Y. Kuo[†] Dirk Nuyens[‡] Graham Pash[§]
Ian H. Sloan[†] Karen E. Willcox[§]

September 2025

Abstract

We study the application of a quasi-Monte Carlo (QMC) method to a class of semi-linear parabolic reaction-diffusion partial differential equations used to model tumor growth. Mathematical models of tumor growth are largely phenomenological in nature, capturing infiltration of the tumor into surrounding healthy tissue, proliferation of the existing tumor, and patient response to therapies, such as chemotherapy and radiotherapy. Considerable inter-patient variability, inherent heterogeneity of the disease, sparse and noisy data collection, and model inadequacy all contribute to significant uncertainty in the model parameters. It is crucial that these uncertainties can be efficiently propagated through the model to compute quantities of interest (QoIs), which in turn may be used to inform clinical decisions. We show that QMC methods can be successful in computing expectations of meaningful QoIs. Well-posedness results are developed for the model and used to show a theoretical error bound for the case of uniform random fields. The theoretical linear error rate, which is superior to that of standard Monte Carlo, is verified numerically. Encouraging computational results are also provided for lognormal random fields, prompting further theoretical development.

Key words. uncertainty quantification, quasi-Monte Carlo methods, semi-linear parabolic equations, nonlinear analysis, computational oncology

MSC codes. 65D30, 65D32, 92B05, 92C50, 35K58

1 Introduction

Uncertainty quantification (UQ) is crucial in precision medicine, establishing trust in computational models for high-consequence applications. This is particularly salient in oncology, where

*ADG, FYK, and IHS acknowledge financial support from the Australian Research Council Discovery Project (DP240100769). DN acknowledges funding from Research Foundation Flanders (FWO G091920N). FYK, DN, and IHS acknowledge support from the J. Tinsley Oden Faculty Fellowship Research Program. GP and KW acknowledge support from Department of Energy grant DE-SC002317 and NSF FDT-Biotech award 2436499. The authors acknowledge the Texas Advanced Computing Center (TACC) at The University of Texas at Austin for providing computational resources (Lonestar6) which contributed to the research results reported within this paper.

[†]School of Mathematics and Statistics, UNSW Sydney, Sydney NSW 2052, Australia (alexander.gilbert@unsw.edu.au, f.kuo@unsw.edu.au, i.sloan@unsw.edu.au).

[‡]Department of Computer Science, KU Leuven, Belgium. (dirk.nuyens@kuleuven.be).

[§]Oden Institute for Computational Engineering and Sciences, University of Texas at Austin, Austin, TX 78712 USA (gtpash@utexas.edu, kwillcox@oden.utexas.edu).

biomedical imaging plays a critical role in the diagnosis and management of a variety of tumors. However, these data are noisy, infrequently collected, and only indirectly informative, all contributing to significant uncertainty in calibrated models. Practical decision making requires efficient methods for the forward propagation of this uncertainty through mathematical and computational models as well as the estimation of clinically relevant quantity of interests (QoIs). In this work, we develop quasi-Monte Carlo (QMC) methods for efficiently estimating the expectation of QoIs from non-linear partial differential equation (PDE) models of tumor growth.

We consider a semi-linear parabolic reaction-diffusion PDE model of tumor growth that captures both invasion into surrounding tissue [1] and proliferation of the existing lesion [5]. This is an established model in the field of computational oncology [44] and has been extended to account for patient response to systemic chemo-radiation therapy [25]. Here, we model the uncertain diffusion and proliferation coefficients as random fields, the uncertainty in which leads to uncertainty in the modeled state and QoIs. We will consider the expectation to be integrated over finitely many random variables by truncating a series expansion representing the formally infinite-dimensional input random fields to a sum over finitely many terms. To efficiently address the high-dimensional integral, we will employ QMC methods with the aim of improving upon the slow convergence of standard Monte Carlo (MC) simulation.

QMC methods are a class of quadrature rules designed to compute high-dimensional integrals (or equivalently expectations). The key benefits of QMC methods are that they can be tailored to achieve dimension-independent error bounds with faster than MC convergence rates for smooth integrands. QMC methods have demonstrated impressive performance in several UQ applications involving PDEs with random coefficients or domains, such as linear elliptic PDEs [12, 15, 18, 19, 20, 22, 29], elliptic eigenvalue problems [17, 37] and more recently linear parabolic equations with control [21]. However, much of the theory has focused on *linear* PDEs. The present work extends the theory in the case of *non-linear*, specifically *semi-linear*, *parabolic* equations, providing a roadmap for adapting QMC methods to wider classes of applications. Apart from the above work on eigenvalue problems[1], to the best of our knowledge this paper is the first to analyze QMC methods for a non-linear PDE.

Well-posedness results are developed for the parametric PDE model in general. Rigorous error estimates are proven for the special case of uniform random fields and confirmed with numerical experiments. Note that we do not analyze the error originating from the spatio-temporal discretization of the governing PDE, leaving this for future work. Encouraging numerical results are also presented for a more realistic test case of log-normal random fields on a complex, unstructured domain, used previously in models of gliomas in the brain [30, 38].

One of our key intermediate results in the QMC error analysis is a bound on the derivatives of the solution with respect to uniform random parameters. Similar parametric regularity results have also been studied for related classes of semi-linear elliptic PDEs in [7, 23, 24]; see also e.g., [2, 8] for other nonlinear PDE or SPDE.

However, the nonlinear term considered here, namely, $u(1-u)$ (see (2.1)), does not fit the settings in [7, 23, 24]. In particular, it is not monotone and so requires a novel proof, which uses the property that if our initial condition lies in $[0, 1]$ then the solution remains in $[0, 1]$ (proven in Section 2.5). We also makes use of the falling factorial combinatorial bound from [6]. We stress that obtaining regularity bounds for parabolic (time-dependent) nonlinear problems here is significantly harder than for elliptic problems in [6, 7, 23, 24] due to the need to handle both space and time derivatives and integrals in the norms. The parametric regularity bounds presented here are also of independent interest beyond QMC since they are often required to analyze other parametric approximation methods, e.g., sparse grids or stochastic collocation.

The remainder of this paper is organized as follows. In Section 2 we present the governing equations and variational framework, and then establish well-posedness and an *a priori* bound

[1] While eigenvalue problems are also nonlinear, the differential operators [17, 37] are linear.

with explicit constant depending on the parameters for general random field models. A parametric regularity bound is obtained for the case of uniform random fields in Section 3. Our main result addresses the QMC error rate in Section 4. The theoretical results are confirmed with supporting numerical experiments in Section 5. Conclusions are drawn in Section 6.

2 Problem formulation

2.1 Governing equation

The invasion of a solid tumor into surrounding healthy tissue is typically modeled as a diffusion process, while the proliferation of existing tumor is modeled with logistic growth subject to some carrying capacity. These phenomenological assumptions give rise to a semi-linear parabolic reaction-diffusion PDE [36], which has demonstrated predictive value for a variety of solid tumors [9, 26, 27, 33]. The model is given by

$$\text{PDE I:} \quad \begin{cases} \dfrac{\partial u}{\partial t} - \nabla \cdot (a \nabla u) - \kappa\, u\,(1-u) + f\,u = 0, & \boldsymbol{x} \in \Omega, \quad t \in I, \\ u(\boldsymbol{x},0) = u_0(\boldsymbol{x}), & \boldsymbol{x} \in \Omega \\ \nabla u \cdot \boldsymbol{n} = 0, & \boldsymbol{x} \in \partial\Omega, \quad t \in I, \end{cases} \tag{2.1}$$

where $u = u^{\boldsymbol{y}}(\boldsymbol{x},t)$ models the *tumor volume fraction* varying in time t on the interval $I := [0,T]$ and over spatial coordinates $\boldsymbol{x} \in \Omega$, where $\Omega \subset \mathbb{R}^d$ is the bounded spatial domain with physical dimension $d \in \{2,3\}$ and Lipschitz boundary $\partial\Omega$ with outward unit normal $\boldsymbol{n}$. The homogeneous Neumann boundary condition ensures that the tumor does not grow beyond the boundary of the domain. The linear reaction term $f\,u$ models the effect of treatment. The initial tumor volume fraction $u_0(\boldsymbol{x})$ may be estimated from medical imaging data. It is natural to assume

$$0 \le u_0(\boldsymbol{x}) \le 1 \qquad \text{for all } \boldsymbol{x} \in \Omega. \tag{2.2}$$

Systemic therapies, such as chemotherapy and radiotherapy form the basis of many treatment protocols, for example, gliomas in the brain [43]. Combination chemoradiation may be modeled as a linear effect on the state, $f = f(\boldsymbol{x},t) = f_{\rm rt}(\boldsymbol{x},t) + f_{\rm ct}(\boldsymbol{x},t)$, with

$$f_{\rm rt}(\boldsymbol{x},t) = \gamma_{{\rm rt},\varepsilon} \sum_k \left[1 - \exp(-\alpha_{\rm rt}\, z_{{\rm rt},k}(\boldsymbol{x}) - \beta_{\rm rt}\, z_{{\rm rt},k}^2(\boldsymbol{x}))\right] \mathbb{1}(t \in [t_{{\rm rt},k}, t_{{\rm rt},k} + \varepsilon]), \tag{2.3}$$

$$f_{\rm ct}(\boldsymbol{x},t) = \alpha_{\rm ct} \sum_\ell z_{{\rm ct},\ell}(\boldsymbol{x}) \exp(-\beta_{\rm ct}(t - \tau_{{\rm ct},\ell}))\, \mathbb{1}(t \ge \tau_{{\rm ct},\ell}), \tag{2.4}$$

where $\mathcal{T}_{\rm rt} = \{\tau_{{\rm rt},k}\}_k$ and $\mathcal{T}_{\rm ct} = \{\tau_{{\rm ct},\ell}\}_\ell$ denote the collection of times at which radiotherapy and chemotherapy are administered, respectively, and $\mathbb{1}$ denotes the indicator function. Radiotherapy is assumed to be instantaneous at the moment of treatment with no lasting or time-delaying effects. The application duration is much smaller than the time-discretization, that is, $\varepsilon \ll \Delta t$, where Δt is the step size. The surviving fraction is computed with the linear-quadratic model: $z_{{\rm rt},k}(\boldsymbol{x})$ is the radiotherapy dosage, $\alpha_{\rm rt} > 0$ and $\beta_{\rm rt} > 0$ are parameters describing the radiosensitivity of the tissue, and $\gamma_{{\rm rt},\varepsilon} > 0$ is a parameter that ensures appropriate physical units [3, 35, 40]. Chemotherapy is assumed to follow a decaying exponential model: $z_{{\rm ct},\ell}(\boldsymbol{x})$ is the drug concentration, $\alpha_{\rm ct} > 0$ is the efficacy, and $\beta_{\rm ct} > 0$ is the clearance rate [25, 27].

The superscript $\boldsymbol{y}$ denotes a parametric vector modeling any randomness and we allow time-varying coefficients for the diffusion $a = a^{\boldsymbol{y}}(\boldsymbol{x},t)$ and proliferation $\kappa = \kappa^{\boldsymbol{y}}(\boldsymbol{x},t)$. The precise details on the modeling of the random fields is deferred to Section 3. However, we will restrict the parametric vectors $\boldsymbol{y}$ to some admissible parameter set $U \subset \mathbb{R}^{\mathbb{N}}$, such that

$$\begin{cases} 0 < a_{\min}^{\boldsymbol{y}} \le a^{\boldsymbol{y}}(\boldsymbol{x},t) \le a_{\max}^{\boldsymbol{y}} < \infty, \\ 0 \le \kappa_{\min}^{\boldsymbol{y}} \le \kappa^{\boldsymbol{y}}(\boldsymbol{x},t) \le \kappa_{\max}^{\boldsymbol{y}} < \infty, \\ 0 = f_{\min} \le f(\boldsymbol{x},t) \le f_{\max} < \infty, \end{cases} \qquad \text{for all } \boldsymbol{x} \in \Omega,\ t \in I,\ \boldsymbol{y} \in U. \tag{2.5}$$

2.2 Functional framework

Let $H^1(\Omega)$ denote the usual first-order Sobolev space on Ω with (squared) norm

$$\|v\|_{H^1(\Omega)}^2 := \|v\|_{L^2(\Omega)}^2 + \|\nabla v\|_{L^2(\Omega)}^2.$$

Let $H^1(\Omega)^*$ denote the dual space of $H^1(\Omega)$, i.e., the space of all bounded linear functionals on $H^1(\Omega)$. We denote the duality pairing between $H^1(\Omega)^*$ and $H^1(\Omega)$ by $\langle\cdot,\cdot\rangle_{H^1(\Omega)^*,H^1(\Omega)}$, with $L^2(\Omega) = L^2(\Omega)^*$ as the pivot space. The dual norm is defined by

$$\|z\|_{H^1(\Omega)^*} := \sup_{0\neq v\in H^1(\Omega)} \frac{|\langle z,v\rangle_{H^1(\Omega)^*,H^1(\Omega)}|}{\|v\|_{H^1(\Omega)}} = \sup_{0\neq v\in H^1(\Omega)} \frac{|\int_\Omega z\, v\,\mathrm{d}\boldsymbol{x}|}{\|v\|_{H^1(\Omega)}}.$$

It is advantageous to consider functions of time with values in Banach spaces when dealing with time-dependent problems. For a Banach space B, let the space $L^2(I;B)$ consist of all measurable functions $v : I \to B$ with finite norm $\|v\|_{L^2(I;B)}^2 := \int_I \|v(\cdot,t)\|_B^2\,\mathrm{d}t$, and let $C(I;B)$ consist of all functions $v : I \to B$ that are continuous at every $t \in I$ with norm $\|v\|_{C(I;B)} := \max_{t\in I}\|v(\cdot,t)\|_B$. Specifically, in this paper we make use of the following norms:

$$\begin{aligned}
\|v\|_{L^2(I;L^2(\Omega))}^2 &:= \int_I \|v(\cdot,t)\|_{L^2(\Omega)}^2\,\mathrm{d}t,\\
\|v\|_{L^2(I;H^1(\Omega))}^2 &:= \int_I \|v(\cdot,t)\|_{H^1(\Omega)}^2\,\mathrm{d}t = \int_I \big(\|v(\cdot,t)\|_{L^2(\Omega)}^2 + \|\nabla v(\cdot,t)\|_{L^2(\Omega)}^2\big)\,\mathrm{d}t,\\
\|v\|_{L^2(I;H^1(\Omega)^*)}^2 &:= \int_I \|v(\cdot,t)\|_{H^1(\Omega)^*}^2\,\mathrm{d}t,\\
\|v\|_{C(I;L^2(\Omega))} &:= \max_{t\in I}\|v(\cdot,t)\|_{L^2(\Omega)}.
\end{aligned}$$

Note that $L^2(I;H^1(\Omega))^* = L^2(I;H^1(\Omega)^*)$.

We follow Tröltzsch [45, §3.4] to analyze our PDE solution in the space $\mathcal{X}$ (denoted by $W(0,T)$ in [45]) which consists of all functions $v \in L^2(I;H^1(\Omega))$ with (distributional) derivative $\frac{\partial}{\partial t}v \in L^2(I;H^1(\Omega)^*)$, and we equip the space $\mathcal{X}$ with the (graph) norm

$$\begin{aligned}
\|v\|_{\mathcal{X}}^2 &:= \|v\|_{L^2(I;H^1(\Omega))}^2 + \|\tfrac{\partial}{\partial t}v\|_{L^2(I;H^1(\Omega)^*)}^2\\
&= \int_I \big(\|v(\cdot,t)\|_{H^1(\Omega)}^2 + \|\tfrac{\partial}{\partial t}v(\cdot,t)\|_{H^1(\Omega)^*}^2\big)\,\mathrm{d}t\\
&= \int_I \big(\|v(\cdot,t)\|_{L^2(\Omega)}^2 + \|\nabla v(\cdot,t)\|_{L^2(\Omega)}^2 + \|\tfrac{\partial}{\partial t}v(\cdot,t)\|_{H^1(\Omega)^*}^2\big)\,\mathrm{d}t.
\end{aligned}$$

A fundamental property we will use is that the space $\mathcal{X}$ is embedded in $C(I;L^2(\Omega))$, see [45, Theorems 3.10 and 3.11], and therefore we formally write for $v \in \mathcal{X}$,

$$\int_I\int_\Omega \frac{\partial v}{\partial t} v\,\mathrm{d}\boldsymbol{x}\,\mathrm{d}t = \int_I \frac{1}{2}\frac{\mathrm{d}}{\mathrm{d}t}\|v(\cdot,t)\|_{L^2(\Omega)}^2\,\mathrm{d}t = \frac{\|v(\cdot,T)\|_{L^2(\Omega)}^2 - \|v(\cdot,0)\|_{L^2(\Omega)}^2}{2}.$$

We will make use of a number of embedding constants which we summarize together here:

$$\begin{aligned}
\|v\|_{H^1(\Omega)^*} \le \|v\|_{L^2(\Omega)} &\le \|v\|_{H^1(\Omega)},\\
\|v\|_{L^4(\Omega)} &\le \theta_1\,\|v\|_{H^1(\Omega)}, &(2.6)\\
\|v\|_{C(I;L^2(\Omega))} &\le \theta_2\,\|v\|_{\mathcal{X}}. &(2.7)
\end{aligned}$$

The embedding (2.6) is due to the Sobolev embedding theorem for $H^1(\Omega)$, see e.g., [45, Theorem 7.1], which state that $H^1(\Omega)$ is embedded in $L^p(\Omega)$ when $d = 2$ and $1 \le p < \infty$, and when $d \ge 3$ and $1 \le p \le \frac{2d}{d-2}$.

Another property we will use is that the space $H^1(\Omega)$ is closed under addition, subtraction, and the maximum and minimum operations, see e.g., [16, Lemma 7.6]. This allows us to define continuous piecewise-smooth test functions in $H^1(\Omega)$.

2.3 Reparameterization

In the case where $f = 0$, that is, untreated growth, the PDE model (2.1) is the well-studied Fisher-KPP equation [14, 28], and well-posedness results are readily available, see e.g., [39, §3.10.3]. However, we consider $f \neq 0$, thus standard results are not immediately applicable. PDE I (2.1) can be rewritten as

$$\frac{\partial u}{\partial t} - \nabla \cdot (a \nabla u) + \kappa u^2 + (f - \kappa) u = 0.$$

It is not known *a priori* whether $f \geq \kappa$ holds. Moreover, we are unable to deduce monotonicity of the function $\kappa u^2 + (f - \kappa) u$ with respect to u. Consequently, we cannot claim the existence and uniqueness of a solution using known results, such as those in [45].

Following a standard technique for treating parabolic PDEs involving a linear term with a negative coefficient (see e.g., [13, §7.5 Problem 8]), we use the substitution

$$u^{\boldsymbol{y}}(\boldsymbol{x}, t) = e^{\lambda^{\boldsymbol{y}} t} w^{\boldsymbol{y}}(\boldsymbol{x}, t),$$

for some $\lambda^{\boldsymbol{y}} \in \mathbb{R}$, possibly depending on $\boldsymbol{y}$, to obtain

$$u = e^{\lambda t} w \quad \Longrightarrow \quad \frac{\partial u}{\partial t} = \lambda e^{\lambda t} w + e^{\lambda t} \frac{\partial w}{\partial t} \quad \text{and} \quad \nabla u = e^{\lambda t} \nabla w,$$

where to simplify notation we have omitted the $\boldsymbol{y}$ dependence. Therefore, after dividing through by $e^{\lambda t}$ and regrouping, the PDE becomes

$$\frac{\partial w}{\partial t} - \nabla \cdot (a \nabla w) + \kappa e^{\lambda t} w^2 + (\lambda + f - \kappa) w = 0.$$

Thus we have the reparametrized PDE problem,

$$\text{PDE II:} \quad \begin{cases} \dfrac{\partial w}{\partial t} - \nabla \cdot (a \nabla w) + b w^2 + c w = 0, & \boldsymbol{x} \in \Omega, \quad t \in I, \\ w(\boldsymbol{x}, 0) = w_0(\boldsymbol{x}), & \boldsymbol{x} \in \Omega \\ \nabla w \cdot \boldsymbol{n} = 0, & \boldsymbol{x} \in \partial\Omega, \quad t \in I, \end{cases} \tag{2.8}$$

with coefficients and initial condition related to PDE I (2.1) via

$$\begin{cases} b^{\boldsymbol{y}}(\boldsymbol{x}, t) := \kappa^{\boldsymbol{y}}(\boldsymbol{x}, t) \exp(\lambda^{\boldsymbol{y}} t), \\ c^{\boldsymbol{y}}(\boldsymbol{x}, t) := \lambda^{\boldsymbol{y}} + f(\boldsymbol{x}, t) - \kappa^{\boldsymbol{y}}(\boldsymbol{x}, t), \\ w_0(\boldsymbol{x}) := u_0(\boldsymbol{x}). \end{cases} \tag{2.9}$$

To ensure that $c^{\boldsymbol{y}}(\boldsymbol{x}, t) > 0$, we may take any $\lambda^{\boldsymbol{y}} > \kappa^{\boldsymbol{y}}_{\max}$. From (2.2) we have $0 \leq w_0(\boldsymbol{x}) \leq 1$ for all $\boldsymbol{x} \in \Omega$. It follows from (2.5) that

$$\begin{cases} 0 < a^{\boldsymbol{y}}_{\min} \leq a^{\boldsymbol{y}}(\boldsymbol{x}, t) \leq a^{\boldsymbol{y}}_{\max} < \infty, \\ 0 \leq \kappa^{\boldsymbol{y}}_{\min} \leq b^{\boldsymbol{y}}(\boldsymbol{x}, t) \leq \kappa^{\boldsymbol{y}}_{\max} e^{\lambda^{\boldsymbol{y}} T} < \infty, \\ 0 < \lambda^{\boldsymbol{y}} - \kappa^{\boldsymbol{y}}_{\max} \leq c^{\boldsymbol{y}}(\boldsymbol{x}, t) \leq \lambda^{\boldsymbol{y}} + f_{\max} - \kappa^{\boldsymbol{y}}_{\min} < \infty, \end{cases} \quad \text{for all } \boldsymbol{x} \in \Omega,\ t \in I,\ \boldsymbol{y} \in U. \tag{2.10}$$

2.4 Well-posedness

In this section, we provide an existence and uniqueness result for the system. We begin by deriving the parametric variational formulation of the PDE problem.

For fixed $\boldsymbol{y} \in U$, a function $u^{\boldsymbol{y}} \in \mathcal{X}$ is said to be a weak solution for PDE I (2.1) if

$$\begin{cases} \displaystyle\int_I \int_\Omega \frac{\partial u}{\partial t} v \,\mathrm{d}\boldsymbol{x} \,\mathrm{d}t = -\int_I \int_\Omega a \nabla u \cdot \nabla v \,\mathrm{d}\boldsymbol{x} \,\mathrm{d}t - \int_I \int_\Omega (\kappa u^2 + (f-\kappa) u) v \,\mathrm{d}\boldsymbol{x} \,\mathrm{d}t & \forall v \in \mathcal{X}, \\ \displaystyle\int_\Omega u(\cdot, 0) v \,\mathrm{d}\boldsymbol{x} = \int_\Omega u_0 v \,\mathrm{d}\boldsymbol{x} & \forall v \in L^2(\Omega). \end{cases} \tag{2.11}$$

The first condition was obtained by multiplying the PDE with a test function $v \in \mathcal{X}$, integrating over $\boldsymbol{x} \in \Omega$ and $t \in I$, applying integration by parts on the diffusion term, and noting that $\int_{\partial\Omega} a \nabla u \cdot \boldsymbol{n} v \,\mathrm{d}\boldsymbol{x} = 0$ due to the Neumann boundary condition.

Analogously, a function $w^{\boldsymbol{y}} \in \mathcal{X}$ is said to be a weak solution for PDE II (2.8) if

$$\begin{cases} \displaystyle\int_I \int_\Omega \frac{\partial w}{\partial t} v \,\mathrm{d}\boldsymbol{x} \,\mathrm{d}t = -\int_I \int_\Omega a \nabla w \cdot \nabla v \,\mathrm{d}\boldsymbol{x} \,\mathrm{d}t - \int_I \int_\Omega (b w^2 + c w) v \,\mathrm{d}\boldsymbol{x} \,\mathrm{d}t & \forall v \in \mathcal{X}, \\ \displaystyle\int_\Omega w(\cdot, 0) v \,\mathrm{d}\boldsymbol{x} = \int_\Omega w_0 v \,\mathrm{d}\boldsymbol{x} & \forall v \in L^2(\Omega). \end{cases} \tag{2.12}$$

Theorem 2.1 (existence, uniqueness, boundedness) *For every $\boldsymbol{y} \in U$ and $\lambda^{\boldsymbol{y}} > \kappa_{\max}^{\boldsymbol{y}} \geq 0$, consider PDE II (2.8) with bounded initial condition $w_0 \in L^2(\Omega)$, $0 \leq w_0(\boldsymbol{x}) \leq 1$ for all $\boldsymbol{x} \in \Omega$, and bounded coefficients (2.9)–(2.10). Then, there exists a unique weak solution $w^{\boldsymbol{y}} \in \mathcal{X}$ to PDE II, which is bounded by $0 \leq w^{\boldsymbol{y}}(\boldsymbol{x}, t) \leq e^{-\lambda^{\boldsymbol{y}} t}$ for a.e. $\boldsymbol{x} \in \Omega$ and all $t \in I$, and it satisfies the a priori bound $\|w^{\boldsymbol{y}}\|_{\mathcal{X}} \leq C^{\boldsymbol{y}} \|w_0\|_{L^2(\Omega)}$ with a constant $C^{\boldsymbol{y}} > 0$.*

In turn, $u^{\boldsymbol{y}} = e^{\lambda^{\boldsymbol{y}} t} w^{\boldsymbol{y}} \in \mathcal{X}$ is the unique weak solution to PDE I (2.1) with bounded initial condition $u_0 = w_0 \in L^2(\Omega)$, $0 \leq u_0(\boldsymbol{x}) \leq 1$ for all $\boldsymbol{x} \in \Omega$, and bounded coefficients (2.5), and it is bounded by $0 \leq u^{\boldsymbol{y}}(\boldsymbol{x}, t) \leq 1$ for a.e. $\boldsymbol{x} \in \Omega$ and all $t \in I$.

Before proving this theorem, we first remark that there is considerable theory developed for the case of monotone semi-linear equations [45], which we could readily make use of were the term $b w^2 + c w$ of PDE II (2.8) monotone in w. Unfortunately, $b w^2 + c w$ is generally not monotone, unless it is known that $w \geq 0$. Moreover, recall that the solution for PDE I (2.1) represents the tumor volume fraction and should naturally satisfy $0 \leq u \leq 1$, corresponding to $0 \leq w \leq e^{-\lambda t}$. But these bounds are not immediately obvious. We therefore modify our PDE II by imposing a restriction on the term $b w^2 + c w$ whenever $w < 0$ or $w > e^{-\lambda t}$:

$$\text{PDE III:} \quad \begin{cases} \dfrac{\partial w}{\partial t} - \nabla \cdot (a \nabla w) + d(w) = 0, & \boldsymbol{x} \in \Omega, \quad t \in I, \\ w(\boldsymbol{x}, 0) = w_0(\boldsymbol{x}), & \boldsymbol{x} \in \Omega \\ \nabla w \cdot \boldsymbol{n} = 0, & \boldsymbol{x} \in \partial\Omega, \quad t \in I, \end{cases} \tag{2.13}$$

where we define a continuous piecewise cutoff function

$$d(w) := \begin{cases} 0 & \text{if } w < 0, \\ b w^2 + c w & \text{if } 0 \leq w \leq e^{-\lambda t}, \\ b e^{-2\lambda t} + c e^{-\lambda t} = (\lambda + f) e^{-\lambda t} & \text{if } w > e^{-\lambda t}. \end{cases} \tag{2.14}$$

A weak solution $w^{\boldsymbol{y}} \in \mathcal{X}$ to PDE III (2.13) satisfies (2.12) with $b w^2 + c w$ replaced by $d(w)$.

Our argument for proving Theorem 2.1 goes as follows:

1. For fixed $\boldsymbol{y} \in U$ and $\lambda^{\boldsymbol{y}} > \kappa_{\max}^{\boldsymbol{y}}$, we infer from [45, Assumptions 5.1 and 5.2, Lemmas 5.3 and 7.10] that there exists a unique weak solution $w_*^{\boldsymbol{y}} \in \mathcal{X}$ of PDE III with bounded coefficients (2.10), with *a priori* bound $\|w_*^{\boldsymbol{y}}\|_{\mathcal{X}} \leq C^{\boldsymbol{y}} \|w_0\|_{L^2(\Omega)}$ for $C^{\boldsymbol{y}} > 0$.

2. We prove that if the initial condition satisfies $0 \le w_0(\boldsymbol{x}) \le 1$ for all $\boldsymbol{x} \in \Omega$ then this unique solution $w_*^{\boldsymbol{y}} \in \mathcal{X}$ of PDE III satisfies $0 \le w_*^{\boldsymbol{y}}(\boldsymbol{x}, t) \le e^{-\lambda^{\boldsymbol{y}} t}$ for a.e. $\boldsymbol{x} \in \Omega$ and all $t \in I$.

3. Then, for this unique solution $w_*^{\boldsymbol{y}} \in \mathcal{X}$, PDE III holds with $d(w)$ defined only by the middle case. This shows that $w_*^{\boldsymbol{y}} \in \mathcal{X}$ is also a solution for PDE II. This confirms the existence of a solution for PDE II satisfying $0 \le w_*^{\boldsymbol{y}}(\boldsymbol{x}, t) \le e^{-\lambda^{\boldsymbol{y}} t}$ for a.e. $\boldsymbol{x} \in \Omega$ and all $t \in I$, given the bounded initial condition $0 \le w_0(\boldsymbol{x}) \le 1$ for all $\boldsymbol{x} \in \Omega$.

4. Finally we prove that this solution $w_*^{\boldsymbol{y}} \in \mathcal{X}$ for PDE II is unique, and hence conclude that $u^{\boldsymbol{y}}(\boldsymbol{x}, t) = e^{\lambda^{\boldsymbol{y}} t} w_*^{\boldsymbol{y}}(\boldsymbol{x}, t)$ is the unique solution of PDE I, and it satisfies $0 \le u(\boldsymbol{x}, t) \le 1$ for a.e. $\boldsymbol{x} \in \Omega$ and all $t \in I$.

The strategy of working with a cutoff function in PDE III and using piecewise test functions (see our proof below) appears already in the literature, sometimes referred to as Stampacchia truncation, see e.g., [4, 10, 39, 45]. However, the problem settings in those references differ from ours, so we include a proof for completeness.

Proof. [Proof of Theorem 2.1] We begin by proving the existence of a solution.

EXISTENCE. We fix $\boldsymbol{y} \in U$ and assume bounded coefficients (2.10). We write the cutoff function (2.14) showing explicit dependence on all arguments,

$$d(w) = d(\boldsymbol{x}, t, w) := \begin{cases} 0 & \text{if } w^{\boldsymbol{y}}(x, t) < 0, \\ b^{\boldsymbol{y}}(\boldsymbol{x}, t) \left(w^{\boldsymbol{y}}(\boldsymbol{x}, t)\right)^2 + c^{\boldsymbol{y}}(\boldsymbol{x}, t)\, w^{\boldsymbol{y}}(x, t) & \text{if } 0 \le w^{\boldsymbol{y}}(x, t) \le e^{-\lambda^{\boldsymbol{y}} t}, \\ b^{\boldsymbol{y}}(\boldsymbol{x}, t)\, e^{-2\lambda^{\boldsymbol{y}} t} + c^{\boldsymbol{y}}(\boldsymbol{x}, t)\, e^{-\lambda^{\boldsymbol{y}} t} & \text{if } w^{\boldsymbol{y}}(x, t) > e^{-\lambda^{\boldsymbol{y}} t}. \end{cases}$$

We see that PDE III satisfies [45, Assumption 5.1]: Ω is a bounded Lipschitz domain; for fixed $w \in \mathbb{R}$, the function $d(\boldsymbol{x}, t, w)$ is measurable with respect to $\boldsymbol{x} \in \Omega$ and $t \in I$; for all $\boldsymbol{x} \in \Omega$ and $t \in I$, the function $d(\boldsymbol{x}, t, w)$ is monotonically increasing (nondecreasing) with respect to $w \in \mathbb{R}$. We see that PDE III also satisfies [45, Assumption 5.2]: for all $\boldsymbol{x} \in \Omega$ and $t \in I$, the function $d(\boldsymbol{x}, t, w)$ is uniformly bounded and Lipschitz in $w \in \mathbb{R}$.

Hence, by [45, Lemma 5.3] and subsequent discussions, there exists a unique weak solution of PDE III in $\mathcal{X}$. Consequently, by [45, Lemma 7.10], this solution satisfies $\|w^{\boldsymbol{y}}\|_{\mathcal{X}} \le C^{\boldsymbol{y}} \|w_0\|_{L^2(\Omega)}$ with a constant $C^{\boldsymbol{y}} > 0$.

We proceed to prove that this unique weak solution for PDE III is bounded between 0 and $e^{-\lambda t}$ if the initial condition is bounded by $0 \le w_0(\boldsymbol{x}) \le 1$ for all $\boldsymbol{x} \in \Omega$. Integrating (2.13), using integration by parts on the diffusion term and using the zero Neumann boundary condition, we have for a.e. $t \in I$ and all $v \in H^1(\Omega)$,

$$\int_\Omega \frac{\partial w}{\partial t}\, v \,\mathrm{d}\boldsymbol{x} = -\int_\Omega a \nabla w \cdot \nabla v \,\mathrm{d}\boldsymbol{x} - \int_\Omega d(w)\, v \,\mathrm{d}\boldsymbol{x}. \tag{2.15}$$

LOWER BOUND. We define $v = w_\#(\cdot, t) \in H^1(\Omega)$ to be the "unwanted lower part" of w,

$$w_\#(\boldsymbol{x}, t) := \min(w(\boldsymbol{x}, t), 0) = \begin{cases} w(\boldsymbol{x}, t) & \text{if } w(\boldsymbol{x}, t) < 0, \\ 0 & \text{otherwise.} \end{cases}$$

For a.e. $\boldsymbol{x} \in \Omega$, since $w(\boldsymbol{x}, 0) = w_0(\boldsymbol{x}) \ge 0$, we have $w_\#(\boldsymbol{x}, 0) = 0$ and $\|w_\#(\cdot, 0)\|_{L^2(\Omega)} = 0$. If $w(\boldsymbol{x}, t) < 0$ then

$$\frac{\partial w}{\partial t}\, w_\# = \frac{\partial w_\#}{\partial t}\, w_\#, \quad \nabla w \cdot \nabla w_\# = |\nabla w_\#|^2, \quad d(w)\, w_\# = 0, \tag{2.16}$$

where we used Case 1 of (2.14). On the other hand, if $w(\boldsymbol{x},t) \geq 0$ then $w_\#(\boldsymbol{x},t) = 0$ and the equalities in (2.16) hold trivially. Putting (2.16) into (2.15) gives for a.e. $t \in I$,

$$\frac{1}{2}\frac{\mathrm{d}}{\mathrm{d}t}\|w_\#(\cdot,t)\|^2_{L^2(\Omega)} = \int_\Omega \frac{\partial w_\#}{\partial t}\, w_\# \,\mathrm{d}\boldsymbol{x} = -\int_\Omega a\,|\nabla w_\#|^2 \,\mathrm{d}\boldsymbol{x} \leq 0.$$

We conclude that $\|w_\#(\cdot,t)\|_{L^2(\Omega)}$ is a nonincreasing function of t. Thus $\|w_\#(\cdot,t)\|_{L^2(\Omega)} \leq \|w_\#(\cdot,0)\|_{L^2(\Omega)} = 0$, and hence $w_\#(\boldsymbol{x},t) = 0$ for a.e. $\boldsymbol{x} \in \Omega$, and in turn this yields

$$w(\boldsymbol{x},t) \geq 0 \qquad \text{for a.e. } \boldsymbol{x} \in \Omega \text{ and all } t \in I.$$

Upper bound. Now we define $v = w_\#(\cdot,t) \in H^1(\Omega)$ on the "unwanted upper part" of w,

$$w_\#(\boldsymbol{x},t) := \max(w(\boldsymbol{x},t) - e^{-\lambda t}, 0) = \begin{cases} w(\boldsymbol{x},t) - e^{-\lambda t} & \text{if } w(\boldsymbol{x},t) > e^{-\lambda t}, \\ 0 & \text{otherwise.} \end{cases}$$

For a.e. $\boldsymbol{x} \in \Omega$, since $w(\boldsymbol{x},0) = w_0(\boldsymbol{x}) \leq 1$, we have $w_\#(\boldsymbol{x},0) = 0$ and $\|w_\#(\cdot,0)\|_{L^2(\Omega)} = 0$. If $w(\boldsymbol{x},t) > e^{-\lambda t}$ then $\frac{\partial w_\#}{\partial t} = \frac{\partial w}{\partial t} + \lambda\, e^{-\lambda t}$, and so

$$\frac{\partial w}{\partial t}\, w_\# = \Big(\frac{\partial w_\#}{\partial t} - \lambda\, e^{-\lambda t}\Big) w_\#,\ \nabla w \cdot \nabla w_\# = |\nabla w_\#|^2,\ d(w)\, w_\# = (\lambda + f)\, e^{-\lambda t}\, w_\#, \tag{2.17}$$

where we used Case 3 of (2.14). On the other hand, if $w(\boldsymbol{x},t) \leq e^{-\lambda t}$ then $w_\#(\boldsymbol{x},t) = 0$ and the equalities in (2.17) hold trivially. Putting (2.17) into (2.15) gives for a.e. $t \in I$,

$$\int_\Omega \Big(\frac{\partial w_\#}{\partial t} - \lambda\, e^{-\lambda t}\Big) w_\# \,\mathrm{d}\boldsymbol{x} = -\int_\Omega a\,|\nabla w_\#|^2 \,\mathrm{d}\boldsymbol{x} - \int_\Omega (\lambda + f)\, e^{-\lambda t}\, w_\# \,\mathrm{d}\boldsymbol{x},$$

which yields

$$\frac{1}{2}\frac{\mathrm{d}}{\mathrm{d}t}\|w_\#(\cdot,t)\|^2_{L^2(\Omega)} = \int_\Omega \frac{\partial w_\#}{\partial t}\, w_\# \,\mathrm{d}\boldsymbol{x} = -\int_\Omega a\,|\nabla w_\#|^2 \,\mathrm{d}\boldsymbol{x} - \int_\Omega f\, e^{-\lambda t}\, w_\# \,\mathrm{d}\boldsymbol{x} \leq 0.$$

We conclude that $\|w_\#(\cdot,t)\|^2_{L^2(\Omega)}$ is a nonincreasing function of t. Thus $\|w_\#(\cdot,t)\|_{L^2(\Omega)} \leq \|w_\#(\cdot,0)\|_{L^2(\Omega)} = 0$, and hence $w_\#(\boldsymbol{x},t) = 0$ for a.e. $\boldsymbol{x} \in \Omega$, and in turn this yields

$$w(\boldsymbol{x},t) \leq e^{-\lambda t} \qquad \text{for a.e. } \boldsymbol{x} \in \Omega \text{ and all } t \in I.$$

Uniqueness. We have shown that the unique solution of PDE III satisfies $0 \leq w(\boldsymbol{x},t) \leq e^{-\lambda t}$ when the initial condition satisfies $0 \leq w_0(\boldsymbol{x}) \leq 1$. For this solution, PDE III holds with $d(w)$ defined only by Case 2 in (2.14). Thus, this solution for PDE III is also a solution for PDE II, demonstrating the existence of a solution for PDE II satisfying $0 \leq w(\boldsymbol{x},t) \leq e^{-\lambda t}$.

Suppose that w_1 and w_2 are two solutions for PDE II, both bounded between 0 and $e^{-\lambda t}$. Then from (2.8) we have for a.e. $t \in I$ and all $v \in H^1(\Omega)$,

$$\begin{aligned} \int_\Omega \frac{\partial w_1}{\partial t}\, v \,\mathrm{d}\boldsymbol{x} &= -\int_\Omega a\,\nabla w_1 \cdot \nabla v \,\mathrm{d}\boldsymbol{x} - \int_\Omega (b\, w_1^2 + c\, w_1)\, v \,\mathrm{d}\boldsymbol{x}, \\ \int_\Omega \frac{\partial w_2}{\partial t}\, v \,\mathrm{d}\boldsymbol{x} &= -\int_\Omega a\,\nabla w_2 \cdot \nabla v \,\mathrm{d}\boldsymbol{x} - \int_\Omega (b\, w_2^2 + c\, w_2)\, v \,\mathrm{d}\boldsymbol{x}. \end{aligned}$$

Subtracting the two equations, writing $w_1^2 - w_2^2 = (w_1 + w_2)\,(w_1 - w_2)$, and taking $v = w_1(\cdot,t) - w_2(\cdot,t) \in H^1(\Omega)$, we obtain

$$\begin{aligned} &\frac{1}{2}\frac{\mathrm{d}}{\mathrm{d}t}\|(w_1 - w_2)(\cdot,t)\|^2_{L^2(\Omega)} \\ &= -\int_\Omega a\,|\nabla(w_1 - w_2)|^2 \,\mathrm{d}\boldsymbol{x} - \int_\Omega (b\,(w_1 + w_2) + c)\,(w_1 - w_2)^2 \,\mathrm{d}\boldsymbol{x} \leq 0, \end{aligned}$$

where we used $w_1(\boldsymbol{x},t) \geq 0$ and $w_2(\boldsymbol{x},t) \geq 0$. We conclude that $\|(w_1 - w_2)(\cdot,t)\|_{L^2(\Omega)}$ is nonincreasing for all $t \in I$, and therefore $\|(w_1 - w_2)(\cdot,t)\|_{L^2(\Omega)} \leq \|(w_1 - w_2)(\cdot,0)\|_{L^2(\Omega)} = 0$. Hence $w_1 \equiv w_2$ and the solution (bounded between 0 and $e^{-\lambda t}$) is unique.

Finally, we conclude that $u(\boldsymbol{x},t) = e^{\lambda t}\, w(\boldsymbol{x},t)$ is the unique weak solution of PDE I, and it satisfies $0 \leq u(\boldsymbol{x},t) \leq 1$ for a.e. $\boldsymbol{x} \in \Omega$ and all $t \in I$. □

2.5 A priori bound

Here we derive *a priori* bounds with explicit constants.

Theorem 2.2 (*a priori* bound) *For every $\boldsymbol{y} \in U$, let $u^{\boldsymbol{y}} \in \mathcal{X}$ denote the unique weak solution to PDE I* (2.1) *with bounded initial condition $u_0 \in L^2(\Omega)$, $0 \leq u_0(\boldsymbol{x}) \leq 1$ for all $\boldsymbol{x} \in \Omega$, and bounded coefficients* (2.5)*. For $\lambda^{\boldsymbol{y}} > \kappa^{\boldsymbol{y}}_{\max} \geq 0$, let $w^{\boldsymbol{y}} \in \mathcal{X}$ denote the corresponding solution to PDE II* (2.8)–(2.10)*. Then we have the a priori bounds*

$$\|w^{\boldsymbol{y}}\|_{\mathcal{X}} \leq C^{\boldsymbol{y}}\, \|w_0\|_{L^2(\Omega)}, \qquad C^{\boldsymbol{y}} := \frac{1 + a^{\boldsymbol{y}}_{\max} + \lambda^{\boldsymbol{y}} + f_{\max}}{\sqrt{2\, \min(a^{\boldsymbol{y}}_{\min}, \lambda^{\boldsymbol{y}} - \kappa^{\boldsymbol{y}}_{\max})}},$$

$$\|u^{\boldsymbol{y}}\|_{\mathcal{X}} \leq \sqrt{\max\left(1 + 2\,(\lambda^{\boldsymbol{y}})^2, 2\right)}\, e^{\lambda^{\boldsymbol{y}} T}\, C^{\boldsymbol{y}}\, \|u_0\|_{L^2(\Omega)}.$$

Proof. Recall that the two solutions are related by $u = e^{\lambda t}\, w$, with $0 \leq u \leq 1$ and $0 \leq w \leq e^{-\lambda t}$. From PDE II (2.8), we have for a.e. $t \in I$ and all $v \in H^1(\Omega)$,

$$\int_\Omega \frac{\partial w}{\partial t}\, v \,\mathrm{d}\boldsymbol{x} = -\int_\Omega a\, \nabla w \cdot \nabla v \,\mathrm{d}\boldsymbol{x} - \int_\Omega (b\, w^2 + c\, w)\, v \,\mathrm{d}\boldsymbol{x}. \tag{2.18}$$

Time derivative. Since $0 \leq w \leq e^{-\lambda t}$, we have $0 \leq b\, w^2 + c\, w \leq (b\, e^{-\lambda t} + c)\, w = (\lambda + f)\, w$ and $|(b\, w^2 + c\, w) v| \leq (\lambda + f)\, w\, |v|$. Thus we obtain from (2.18)

$$\begin{aligned}\Big| \int_\Omega \frac{\partial w}{\partial t}\, v \,\mathrm{d}\boldsymbol{x} \Big| &\leq a_{\max}\, \|\nabla w(\cdot,t)\|_{L^2(\Omega)}\, \|\nabla v\|_{L^2(\Omega)} + (\lambda + f_{\max})\, \|w(\cdot,t)\|_{L^2(\Omega)}\, \|v\|_{L^2(\Omega)} \\ &\leq (a_{\max} + \lambda + f_{\max})\, \|w(\cdot,t)\|_{H^1(\Omega)}\, \|v\|_{H^1(\Omega)},\end{aligned}$$

and therefore

$$\|\tfrac{\partial w}{\partial t}(\cdot,t)\|_{H^1(\Omega)^*} = \sup_{0 \neq v \in H^1(\Omega)} \frac{|\int_\Omega \frac{\partial w}{\partial t}\, v \,\mathrm{d}\boldsymbol{x}|}{\|v\|_{H^1(\Omega)}} \leq (a_{\max} + \lambda + f_{\max})\, \|w(\cdot,t)\|_{H^1(\Omega)},$$

which yields

$$\|\tfrac{\partial}{\partial t} w\|_{L^2(I;H^1(\Omega)^*)} \leq (a_{\max} + \lambda + f_{\max})\, \|w\|_{L^2(I;H^1(\Omega))}. \tag{2.19}$$

Gradient. Taking $v = w(\cdot,t)$ in (2.18) and integrating with respect to $t \in I$, we obtain

$$\begin{aligned}&\frac{\|w(\cdot,T)\|^2_{L^2(\Omega)} - \|w(\cdot,0)\|^2_{L^2(\Omega)}}{2} = \int_I \frac{1}{2} \frac{\mathrm{d}}{\mathrm{d}t} \|w(\cdot,t)\|^2_{L^2(\Omega)} \,\mathrm{d}t \\ &= \int_I \int_\Omega \frac{\partial w}{\partial t}\, w \,\mathrm{d}\boldsymbol{x} \,\mathrm{d}t = -\int_I \int_\Omega a\, |\nabla w|^2 \,\mathrm{d}\boldsymbol{x} \,\mathrm{d}t - \int_I \int_\Omega (b\, w^2 + c\, w)\, w \,\mathrm{d}\boldsymbol{x} \,\mathrm{d}t,\end{aligned}$$

which rearranges into

$$\frac{\|w(\cdot,T)\|^2_{L^2(\Omega)}}{2} + \int_I \int_\Omega a\, |\nabla w|^2 \,\mathrm{d}\boldsymbol{x} \,\mathrm{d}t + \int_I \int_\Omega (b\, w^2 + c\, w)\, w \,\mathrm{d}\boldsymbol{x} \,\mathrm{d}t = \frac{\|w(\cdot,0)\|^2_{L^2(\Omega)}}{2}.$$

Since $0 \le w \le e^{-\lambda t}$, we have $(b\,w^2 + c\,w)\,w \ge c\,w^2$. This yields

$$\begin{aligned}
&\min(a_{\min}, c_{\min})\,\|w\|^2_{L^2(I;H^1(\Omega))} \\
&\le a_{\min} \int_I \|\nabla w(\cdot,t)\|^2_{L^2(\Omega)}\,\mathrm{d}t + c_{\min} \int_I \|w(\cdot,t)\|^2_{L^2(\Omega)}\,\mathrm{d}t \le \frac{\|w_0\|^2_{L^2(\Omega)}}{2},
\end{aligned}$$

with $c_{\min} := \lambda - \kappa_{\max} > 0$, and therefore

$$\|w\|_{L^2(I;H^1(\Omega))} \le \frac{\|w_0\|_{L^2(\Omega)}}{\sqrt{2\,\min(a_{\min}, \lambda - \kappa_{\max})}}. \tag{2.20}$$

A PRIORI BOUND. Combining (2.19) and (2.20), we obtain

$$\begin{aligned}
\|w\|_{\mathcal{X}} &= \sqrt{\|w\|^2_{L^2(I;H^1(\Omega))} + \|\tfrac{\partial}{\partial t} w\|^2_{L^2(I;H^1(\Omega)^*)}} \le \|w\|_{L^2(I;H^1(\Omega))} + \|\tfrac{\partial}{\partial t} w\|_{L^2(I;H^1(\Omega)^*)} \\
&\le (1 + a_{\max} + \lambda + f_{\max})\,\|w\|_{L^2(I;H^1(\Omega))} \le \frac{1 + a_{\max} + \lambda + f_{\max}}{\sqrt{2\,\min(a_{\min}, \lambda - \kappa_{\max})}}\,\|w_0\|_{L^2(\Omega)}.
\end{aligned}$$

Now since $u = e^{\lambda t}\,w$, we have

$$\|u\|^2_{\mathcal{X}} = \int_I \Big(\big\|e^{\lambda t}\,w(\cdot,t)\big\|^2_{L^2(\Omega)} + \big\|\nabla e^{\lambda t}\,w(\cdot,t)\big\|^2_{L^2(\Omega)} + \big\|\tfrac{\partial}{\partial t}[e^{\lambda t}\,w(\cdot,t)]\big\|^2_{H^1(\Omega)^*} \Big)\,\mathrm{d}t,$$

where we can take out a factor $e^{2\lambda t}$ from the first two squared norms on the right-hand side, while the third squared norm can be bounded by

$$\begin{aligned}
\big\|\tfrac{\partial}{\partial t}[e^{\lambda t}\,w(\cdot,t)]\big\|^2_{H^1(\Omega)^*} &= \big\|\lambda\,e^{\lambda t}\,w(\cdot,t) + e^{\lambda t}\,\tfrac{\partial}{\partial t} w(\cdot,t)\big\|^2_{H^1(\Omega)^*} \\
&\le 2\,e^{2\lambda t}\big(\lambda^2\,\|w(\cdot,t)\|^2_{H^1(\Omega)^*} + \|\tfrac{\partial}{\partial t} w(\cdot,t)\|^2_{H^1(\Omega)^*}\big),
\end{aligned}$$

where $\|w(\cdot,t)\|_{H^1(\Omega)^*} \le \|w(\cdot,t)\|_{L^2(\Omega)}$. This yields $\|u\|_{\mathcal{X}} \le \sqrt{\max(1+2\lambda^2, 2)}\,e^{\lambda T}\,\|w\|_{\mathcal{X}}$. $\square$

3 Parametric regularity

3.1 Uniform random field model

We model the coefficients as affine series expansions in terms of uniform parameters $\boldsymbol{y} \in [-\frac{1}{2}, \frac{1}{2}]^{\mathbb{N}}$, see e.g., [21, 29],

$$a^{\boldsymbol{y}}(\boldsymbol{x},t) := \psi_0(\boldsymbol{x},t) + \sum_{j\ge1} y_j\,\psi_j(\boldsymbol{x},t), \tag{3.1}$$

$$\kappa^{\boldsymbol{y}}(\boldsymbol{x},t) := \xi_0(\boldsymbol{x},t) + \sum_{j\ge1} y_j\,\xi_j(\boldsymbol{x},t), \tag{3.2}$$

and both of them are bounded independently of $\boldsymbol{y}$,

$$\begin{aligned}
0 < a_{\min} &:= \|\psi_0\|_\infty - \frac{1}{2}\sum_{j\ge1}\|\psi_j\|_\infty < a_{\max} := \|\psi_0\|_\infty + \frac{1}{2}\sum_{j\ge1}\|\psi_j\|_\infty < \infty, \\
0 < \kappa_{\min} &:= \|\xi_0\|_\infty - \frac{1}{2}\sum_{j\ge1}\|\xi_j\|_\infty < \kappa_{\max} := \|\xi_0\|_\infty + \frac{1}{2}\sum_{j\ge1}\|\xi_j\|_\infty < \infty,
\end{aligned}$$

where we define

$$\|v\|_\infty := \max_{t\in I}\|v(\cdot,t)\|_{L^\infty(\Omega)}.$$

To make the two random fields completely independent, we will later define $\psi_j \equiv 0$ when j is even and $\xi_j \equiv 0$ when j is odd. This can be interpreted as interleaving two series expansions.

Recall it is necessary that $\lambda > \kappa_{\max} \geq 0$, which in this case is independent of $\boldsymbol{y}$. Then, the coefficients in PDE II are

$$b^{\boldsymbol{y}}(\boldsymbol{x},t) := \kappa^{\boldsymbol{y}}(\boldsymbol{x},t)\, e^{\lambda t} = \Big(\xi_0(\boldsymbol{x},t) + \sum_{j\geq 1} y_j\, \xi_j(\boldsymbol{x},t)\Big)\, e^{\lambda t}, \tag{3.3}$$

$$c^{\boldsymbol{y}}(\boldsymbol{x},t) := \lambda + f(\boldsymbol{x},t) - \kappa^{\boldsymbol{y}}(\boldsymbol{x},t) = \lambda + f(\boldsymbol{x},t) - \Big(\xi_0(\boldsymbol{x},t) + \sum_{j\geq 1} y_j\, \xi_j(\boldsymbol{x},t)\Big). \tag{3.4}$$

3.2 Parametric regularity for uniform random fields

We will write derivatives with respect to the parameters $\boldsymbol{y}$ using multiindex notation, where for a multiindex $\boldsymbol{\nu} \in \mathbb{N}^{\mathbb{N}}$ with $|\boldsymbol{\nu}| := \sum_{j\geq 1} \nu_j < \infty$, we define the derivative of order $\boldsymbol{\nu}$ by

$$\partial^{\boldsymbol{\nu}}_{\boldsymbol{y}} = \prod_{j\geq 1} \Big(\frac{\partial}{\partial y_j}\Big)^{\nu_j}.$$

We will use the *absolute value of the falling factorial* as introduced in Chernov and Lê [6, 7]

$$[\tfrac{1}{2}]_0 := 1, \qquad [\tfrac{1}{2}]_n := \big|\tfrac{1}{2}\,(\tfrac{1}{2}-1)\,(\tfrac{1}{2}-2)\cdots(\tfrac{1}{2}-n+1)\big| \quad \text{for } n \geq 1,$$

with $[\frac{1}{2}]_n \leq n! \leq 2\cdot 2^n\,[\frac{1}{2}]_n$, and we will use a key property from [7, Lemma 2.3],

$$\sum_{\boldsymbol{0}\neq \boldsymbol{m}<\boldsymbol{\nu}} \binom{\boldsymbol{\nu}}{\boldsymbol{m}}\, [\tfrac{1}{2}]_{|\boldsymbol{m}|}\, [\tfrac{1}{2}]_{|\boldsymbol{\nu}-\boldsymbol{m}|} \leq 2\,[\tfrac{1}{2}]_{|\boldsymbol{\nu}|}, \tag{3.5}$$

where $\boldsymbol{m} < \boldsymbol{\nu}$ means that $m_j \leq \nu_j$ for all $j \geq 1$, and $\binom{\boldsymbol{\nu}}{\boldsymbol{m}} = \prod_{j\geq 1}\binom{\nu_j}{m_j}$ is a product of binomial coefficients.

Theorem 3.1 (parametric regularity) *For every $\boldsymbol{y} \in U$, let $u^{\boldsymbol{y}} \in \mathcal{X}$ denote the unique weak solution to PDE I* (2.1) *with bounded initial condition $u_0 \in L^2(\Omega)$, $0 \leq u_0(\boldsymbol{x}) \leq 1$ for all $\boldsymbol{x} \in \Omega$, and bounded coefficients* (2.5). *For $\lambda^{\boldsymbol{y}} > \kappa^{\boldsymbol{y}}_{\max} \geq 0$, let $w^{\boldsymbol{y}} \in \mathcal{X}$ denote the corresponding solution to PDE II* (2.8)–(2.10). *Then for every multiindex $\boldsymbol{\nu}$, the $\boldsymbol{\nu}$-th derivative with respect to $\boldsymbol{y}$ of the solutions satisfy the regularity bounds*

$$\|\partial^{\boldsymbol{\nu}}_{\boldsymbol{y}} w^{\boldsymbol{y}}\|_{\mathcal{X}} \leq \max(C, \tfrac{E}{\rho})\,(\rho\,\boldsymbol{\beta})^{\boldsymbol{\nu}}\,[\tfrac{1}{2}]_{|\boldsymbol{\nu}|}\,\|w_0\|_{L^2(\Omega)},$$
$$\|\partial^{\boldsymbol{\nu}}_{\boldsymbol{y}} u^{\boldsymbol{y}}\|_{\mathcal{X}} \leq \widetilde{C}\,(\rho\,\boldsymbol{\beta})^{\boldsymbol{\nu}}\,[\tfrac{1}{2}]_{|\boldsymbol{\nu}|}\,\|u_0\|_{L^2(\Omega)}, \qquad \widetilde{C} := \sqrt{\max(1+2\lambda^2, 2)}\, e^{\lambda T}\, \max(C, \tfrac{E}{\rho}),$$

with the sequence

$$\beta_j := \max(\|\psi_j\|_\infty, \|\xi_j\|_\infty),$$

where C is defined in Theorem 2.2, while E and ρ are defined in (3.20) *and* (3.21) *below, respectively, both depending on Φ defined in* (3.18) *below.*

Proof. For any multiindex $\boldsymbol{\nu} \neq \boldsymbol{0}$, we have the mixed derivative $\partial^{\boldsymbol{\nu}}_{\boldsymbol{y}}$ of (3.1)–(3.4)

$$\partial^{\boldsymbol{\nu}}_{\boldsymbol{y}} a^{\boldsymbol{y}}(\boldsymbol{x},t) = \begin{cases} \psi_j(\boldsymbol{x},t) & \text{if } \boldsymbol{\nu} = \boldsymbol{e}_j \\ 0 & \text{otherwise,} \end{cases} \tag{3.6}$$

$$\partial^{\boldsymbol{\nu}}_{\boldsymbol{y}} b^{\boldsymbol{y}}(\boldsymbol{x},t) = \begin{cases} \xi_j(\boldsymbol{x},t)\, e^{\lambda t} & \text{if } \boldsymbol{\nu} = \boldsymbol{e}_j \\ 0 & \text{otherwise,} \end{cases} \tag{3.7}$$

$$\partial^{\boldsymbol{\nu}}_{\boldsymbol{y}} c^{\boldsymbol{y}}(\boldsymbol{x},t) = \begin{cases} -\xi_j(\boldsymbol{x},t) & \text{if } \boldsymbol{\nu} = \boldsymbol{e}_j \\ 0 & \text{otherwise.} \end{cases} \tag{3.8}$$

Recall that the weak solution $w \in \mathcal{X}$ satisfies (2.12). For any multiindex $\boldsymbol{\nu} \neq \mathbf{0}$ we take the mixed derivative $\partial_{\boldsymbol{y}}^{\boldsymbol{\nu}}$ on both sides of the first condition in (2.12) and use the Leibniz product rule to obtain for all $v \in \mathcal{X}$,

$$\begin{aligned}
\int_I \int_\Omega \frac{\partial}{\partial t}(\partial_{\boldsymbol{y}}^{\boldsymbol{\nu}} w)\, v \,\mathrm{d}\boldsymbol{x}\,\mathrm{d}t = &- \int_I \int_\Omega \sum_{\boldsymbol{k} \le \boldsymbol{\nu}} \binom{\boldsymbol{\nu}}{\boldsymbol{k}} (\partial_{\boldsymbol{y}}^{\boldsymbol{k}} a)\, \nabla(\partial_{\boldsymbol{y}}^{\boldsymbol{\nu}-\boldsymbol{k}} w) \cdot \nabla v \,\mathrm{d}\boldsymbol{x}\,\mathrm{d}t \\
&- \int_I \int_\Omega \sum_{\boldsymbol{k} \le \boldsymbol{\nu}} \binom{\boldsymbol{\nu}}{\boldsymbol{k}} (\partial_{\boldsymbol{y}}^{\boldsymbol{k}} b)\, (\partial_{\boldsymbol{y}}^{\boldsymbol{\nu}-\boldsymbol{k}} w^2)\, v \,\mathrm{d}\boldsymbol{x}\,\mathrm{d}t \\
&- \int_I \int_\Omega \sum_{\boldsymbol{k} \le \boldsymbol{\nu}} \binom{\boldsymbol{\nu}}{\boldsymbol{k}} (\partial_{\boldsymbol{y}}^{\boldsymbol{k}} c)\, (\partial_{\boldsymbol{y}}^{\boldsymbol{\nu}-\boldsymbol{k}} w)\, v \,\mathrm{d}\boldsymbol{x}\,\mathrm{d}t,
\end{aligned} \tag{3.9}$$

where the mixed derivative of w^2 can be expanded further using the Leibniz product rule as

$$(\partial_{\boldsymbol{y}}^{\boldsymbol{\nu}-\boldsymbol{k}} w^2) = \sum_{\boldsymbol{m} \le \boldsymbol{\nu}-\boldsymbol{k}} \binom{\boldsymbol{\nu}-\boldsymbol{k}}{\boldsymbol{m}} (\partial_{\boldsymbol{y}}^{\boldsymbol{m}} w)\, (\partial_{\boldsymbol{y}}^{\boldsymbol{\nu}-\boldsymbol{k}-\boldsymbol{m}} w),$$

for which the $\boldsymbol{k} = \mathbf{0}$ case can be written as

$$(\partial_{\boldsymbol{y}}^{\boldsymbol{\nu}} w^2) = \sum_{\boldsymbol{m} \le \boldsymbol{\nu}} \binom{\boldsymbol{\nu}}{\boldsymbol{m}} (\partial_{\boldsymbol{y}}^{\boldsymbol{m}} w)\, (\partial_{\boldsymbol{y}}^{\boldsymbol{\nu}-\boldsymbol{m}} w) = 2\,(\partial_{\boldsymbol{y}}^{\boldsymbol{\nu}} w)\, w + \sum_{\mathbf{0} \neq \boldsymbol{m} < \boldsymbol{\nu}} \binom{\boldsymbol{\nu}}{\boldsymbol{m}} (\partial_{\boldsymbol{y}}^{\boldsymbol{m}} w)\, (\partial_{\boldsymbol{y}}^{\boldsymbol{\nu}-\boldsymbol{m}} w).$$

Separating out the $\boldsymbol{k} = \mathbf{0}$ terms in (3.9), applying (3.6)–(3.8), and rearranging to have the highest-order mixed derivative $\partial_{\boldsymbol{y}}^{\boldsymbol{\nu}} w$ on the left-hand side, we obtain

$$\begin{aligned}
&\int_I \int_\Omega \frac{\partial}{\partial t}(\partial_{\boldsymbol{y}}^{\boldsymbol{\nu}} w)\, v \,\mathrm{d}\boldsymbol{x}\,\mathrm{d}t \\
&\quad + \int_I \int_\Omega a\, \nabla(\partial_{\boldsymbol{y}}^{\boldsymbol{\nu}} w) \cdot \nabla v \,\mathrm{d}\boldsymbol{x}\,\mathrm{d}t + \int_I \int_\Omega 2\, b\, (\partial_{\boldsymbol{y}}^{\boldsymbol{\nu}} w)\, w\, v \,\mathrm{d}\boldsymbol{x}\,\mathrm{d}t + \int_I \int_\Omega c\, (\partial_{\boldsymbol{y}}^{\boldsymbol{\nu}} w)\, v \,\mathrm{d}\boldsymbol{x}\,\mathrm{d}t \\
&= - \sum_{j \ge 1} \nu_j \int_I \int_\Omega \psi_j\, \nabla(\partial_{\boldsymbol{y}}^{\boldsymbol{\nu}-\boldsymbol{e}_j} w) \cdot \nabla v \,\mathrm{d}\boldsymbol{x}\,\mathrm{d}t + \sum_{j \ge 1} \nu_j \int_I \int_\Omega \xi_j\, (\partial_{\boldsymbol{y}}^{\boldsymbol{\nu}-\boldsymbol{e}_j} w)\, v \,\mathrm{d}\boldsymbol{x}\,\mathrm{d}t \\
&\quad - \sum_{\mathbf{0} \neq \boldsymbol{m} < \boldsymbol{\nu}} \binom{\boldsymbol{\nu}}{\boldsymbol{m}} \int_I \int_\Omega b\, (\partial_{\boldsymbol{y}}^{\boldsymbol{m}} w)\, (\partial_{\boldsymbol{y}}^{\boldsymbol{\nu}-\boldsymbol{m}} w)\, v \,\mathrm{d}\boldsymbol{x}\,\mathrm{d}t \\
&\quad - \sum_{j \ge 1} \nu_j \sum_{\boldsymbol{m} \le \boldsymbol{\nu}-\boldsymbol{e}_j} \binom{\boldsymbol{\nu}-\boldsymbol{e}_j}{\boldsymbol{m}} \int_I \int_\Omega \xi_j\, e^{\lambda t}\, (\partial_{\boldsymbol{y}}^{\boldsymbol{m}} w)\, (\partial_{\boldsymbol{y}}^{\boldsymbol{\nu}-\boldsymbol{e}_j-\boldsymbol{m}} w)\, v \,\mathrm{d}\boldsymbol{x}\,\mathrm{d}t.
\end{aligned} \tag{3.10}$$

Gradient. Taking the mixed derivative $\partial_{\boldsymbol{y}}^{\boldsymbol{\nu}}$ on both sides of the second condition in (2.12) and then taking $v = \partial_{\boldsymbol{y}}^{\boldsymbol{\nu}} w(\cdot, 0)$, we conclude that $\|\partial_{\boldsymbol{y}}^{\boldsymbol{\nu}} w(\cdot,0)\|_{L^2(\Omega)}^2 = 0$. This yields

$$\int_I \int_\Omega \frac{\partial}{\partial t}(\partial_{\boldsymbol{y}}^{\boldsymbol{\nu}} w)\, (\partial_{\boldsymbol{y}}^{\boldsymbol{\nu}} w) \,\mathrm{d}\boldsymbol{x}\,\mathrm{d}t = \int_I \frac{1}{2} \frac{\mathrm{d}}{\mathrm{d}t} \|\partial_{\boldsymbol{y}}^{\boldsymbol{\nu}} w(\cdot,t)\|_{L^2(\Omega)}^2 \,\mathrm{d}t = \frac{\|\partial_{\boldsymbol{y}}^{\boldsymbol{\nu}} w(\cdot,T)\|_{L^2(\Omega)}^2}{2}.$$

Taking $v = \partial_{\boldsymbol{y}}^{\boldsymbol{\nu}} w$ in (3.10) then gives

$$
\begin{aligned}
&\frac{\|\partial_{\boldsymbol{y}}^{\boldsymbol{\nu}} w(\cdot,T)\|_{L^2(\Omega)}^2}{2} + \int_I\int_\Omega a\,|\nabla(\partial_{\boldsymbol{y}}^{\boldsymbol{\nu}} w)|^2\,\mathrm{d}\boldsymbol{x}\,\mathrm{d}t + \int_I\int_\Omega 2\,b\,(\partial_{\boldsymbol{y}}^{\boldsymbol{\nu}} w)^2\,w\,\mathrm{d}\boldsymbol{x}\,\mathrm{d}t + \int_I\int_\Omega c\,(\partial_{\boldsymbol{y}}^{\boldsymbol{\nu}} w)^2\,\mathrm{d}\boldsymbol{x}\,\mathrm{d}t\\
&= -\sum_{j\ge1}\nu_j\int_I\int_\Omega \psi_j\,\nabla(\partial_{\boldsymbol{y}}^{\boldsymbol{\nu}-\boldsymbol{e}_j} w)\cdot\nabla(\partial_{\boldsymbol{y}}^{\boldsymbol{\nu}} w)\,\mathrm{d}\boldsymbol{x}\,\mathrm{d}t + \sum_{j\ge1}\nu_j\int_I\int_\Omega \xi_j\,(\partial_{\boldsymbol{y}}^{\boldsymbol{\nu}-\boldsymbol{e}_j} w)\,(\partial_{\boldsymbol{y}}^{\boldsymbol{\nu}} w)\,\mathrm{d}\boldsymbol{x}\,\mathrm{d}t\\
&\quad - \sum_{\boldsymbol{0}\ne\boldsymbol{m}<\boldsymbol{\nu}}\binom{\boldsymbol{\nu}}{\boldsymbol{m}}\int_I\int_\Omega b\,(\partial_{\boldsymbol{y}}^{\boldsymbol{m}} w)\,(\partial_{\boldsymbol{y}}^{\boldsymbol{\nu}-\boldsymbol{m}} w)\,(\partial_{\boldsymbol{y}}^{\boldsymbol{\nu}} w)\,\mathrm{d}\boldsymbol{x}\,\mathrm{d}t\\
&\quad - \sum_{j\ge1}\nu_j\sum_{\boldsymbol{m}\le\boldsymbol{\nu}-\boldsymbol{e}_j}\binom{\boldsymbol{\nu}-\boldsymbol{e}_j}{\boldsymbol{m}}\int_I\int_\Omega \xi_j\,e^{\lambda t}\,(\partial_{\boldsymbol{y}}^{\boldsymbol{m}} w)\,(\partial_{\boldsymbol{y}}^{\boldsymbol{\nu}-\boldsymbol{e}_j-\boldsymbol{m}} w)\,(\partial_{\boldsymbol{y}}^{\boldsymbol{\nu}} w)\,\mathrm{d}\boldsymbol{x}\,\mathrm{d}t.
\end{aligned}
\tag{3.11}
$$

Until this point we still have equality in (3.11). For the special cases $|\boldsymbol{\nu}| = 1$, the sum over $\boldsymbol{0} \neq \boldsymbol{m} < \boldsymbol{\nu}$ is empty and takes the value 0, with no meaning attached to the summand.

We obtain a lower bound on the left-hand side of (3.11) by dropping some nonnegative terms, including the term with integrand $2\,b\,(\partial_{\boldsymbol{y}}^{\boldsymbol{\nu}} w)^2\,w \ge 0$ since $0 \le w \le e^{-\lambda t}$, so

$$
\begin{aligned}
\mathrm{LHS} &\ge a_{\min}\,\|\nabla(\partial_{\boldsymbol{y}}^{\boldsymbol{\nu}} w)\|_{L^2(I;L^2(\Omega))}^2 + c_{\min}\,\|\partial_{\boldsymbol{y}}^{\boldsymbol{\nu}} w\|_{L^2(I;L^2(\Omega))}^2\\
&\ge \min(a_{\min}, c_{\min})\,\|\partial_{\boldsymbol{y}}^{\boldsymbol{\nu}} w\|_{L^2(I;H^1(\Omega))}^2, \qquad c_{\min} := \lambda - \kappa_{\max} > 0.
\end{aligned}
\tag{3.12}
$$

For the right-hand side of (3.11), we pull out $\beta_j := \max(\|\psi_j\|_\infty, \|\xi_j\|_\infty)$ and then apply the Cauchy–Schwarz inequality to the first two terms, as is typically done. The new challenge is to manage the space-time integrals of three factors involving w in the last two terms of (3.11). If we blindly apply the Cauchy–Schwarz inequality multiple times to separate the three factors, then we would raise norms to higher powers than 2 and the subsequent recursion would fail.

To keep the norms with exponent 2, we apply the generalized Hölder inequality, first for $\boldsymbol{x} \in \Omega$ with $\frac{1}{2} + \frac{1}{4} + \frac{1}{4} = 1$, and then for $t \in I$ with $\frac{1}{\infty} + \frac{1}{2} + \frac{1}{2} = 1$, as follows:

$$
\begin{aligned}
&\int_I\int_\Omega f\,g\,h\,\mathrm{d}\boldsymbol{x}\,\mathrm{d}t \le \int_I \|f\|_{L^2(\Omega)}\,\|g\|_{L^4(\Omega)}\,\|h\|_{L^4(\Omega)}\,\mathrm{d}t\\
&\le \Big(\max_{t\in I}\|f\|_{L^2(\Omega)}\Big)\Big(\int_I \|g\|_{L^4(\Omega)}^2\,\mathrm{d}t\Big)^{1/2}\Big(\int_I \|h\|_{L^4(\Omega)}^2\,\mathrm{d}t\Big)^{1/2}\\
&\le \theta_1^2\Big(\max_{t\in I}\|f\|_{L^2(\Omega)}\Big)\Big(\int_I \|g\|_{H^1(\Omega)}^2\,\mathrm{d}t\Big)^{1/2}\Big(\int_I \|h\|_{H^1(\Omega)}^2\,\mathrm{d}t\Big)^{1/2}\\
&= \theta_1^2\,\|f\|_{C(I;L^2(\Omega))}\,\|g\|_{L^2(I;H^1(\Omega))}\,\|h\|_{L^2(I;H^1(\Omega))} \le \theta_1^2\,\theta_2\,\|f\|_{\mathcal{X}}\,\|g\|_{\mathcal{X}}\,\|h\|_{L^2(I;H^1(\Omega))},
\end{aligned}
\tag{3.13}
$$

where we also used the embeddings (2.6) and (2.7). Hence we obtain from (3.11)–(3.13),

$$
\begin{aligned}
&\min(a_{\min}, \lambda - \kappa_{\max})\,\|\partial_{\boldsymbol{y}}^{\boldsymbol{\nu}} w\|_{L^2(I;H^1(\Omega))}^2\\
&\le \sum_{j\ge1}\nu_j\,\beta_j\,\|\nabla(\partial_{\boldsymbol{y}}^{\boldsymbol{\nu}-\boldsymbol{e}_j} w)\|_{L^2(I;L^2(\Omega))}\,\|\nabla(\partial_{\boldsymbol{y}}^{\boldsymbol{\nu}} w)\|_{L^2(I;L^2(\Omega))}\\
&\quad + \sum_{j\ge1}\nu_j\,\beta_j\,\|\partial_{\boldsymbol{y}}^{\boldsymbol{\nu}-\boldsymbol{e}_j} w\|_{L^2(I;L^2(\Omega))}\,\|\partial_{\boldsymbol{y}}^{\boldsymbol{\nu}} w\|_{L^2(I;L^2(\Omega))}\\
&\quad + \theta_1^2\,\theta_2\,\kappa_{\max}\,e^{\lambda T}\sum_{\boldsymbol{0}\ne\boldsymbol{m}<\boldsymbol{\nu}}\binom{\boldsymbol{\nu}}{\boldsymbol{m}}\|\partial_{\boldsymbol{y}}^{\boldsymbol{m}} w\|_{\mathcal{X}}\,\|\partial_{\boldsymbol{y}}^{\boldsymbol{\nu}-\boldsymbol{m}} w\|_{\mathcal{X}}\,\|\partial_{\boldsymbol{y}}^{\boldsymbol{\nu}} w\|_{L^2(I;H^1(\Omega))}\\
&\quad + \theta_1^2\,\theta_2\,e^{\lambda T}\sum_{j\ge1}\nu_j\,\beta_j\sum_{\boldsymbol{m}\le\boldsymbol{\nu}-\boldsymbol{e}_j}\binom{\boldsymbol{\nu}-\boldsymbol{e}_j}{\boldsymbol{m}}\|\partial_{\boldsymbol{y}}^{\boldsymbol{m}} w\|_{\mathcal{X}}\,\|\partial_{\boldsymbol{y}}^{\boldsymbol{\nu}-\boldsymbol{e}_j-\boldsymbol{m}} w\|_{\mathcal{X}}\,\|\partial_{\boldsymbol{y}}^{\boldsymbol{\nu}} w\|_{L^2(I;H^1(\Omega))},
\end{aligned}
$$

where we used $b \le \kappa_{\max} e^{\lambda T}$. The last factor in every term on the right-hand side can be upper bounded by $\|\partial_{\boldsymbol{y}}^{\boldsymbol{\nu}} w\|_{L^2(I;H^1(\Omega))}$. Canceling out this common factor from both sides and grouping the first two terms on the right-hand side, we arrive at

$$
\begin{aligned}
&\min(a_{\min}, \lambda - \kappa_{\max}) \, \|\partial_{\boldsymbol{y}}^{\boldsymbol{\nu}} w\|_{L^2(I;H^1(\Omega))} \\
&\le 2 \sum_{j\ge 1} \nu_j \, \beta_j \, \|\partial_{\boldsymbol{y}}^{\boldsymbol{\nu}-\boldsymbol{e}_j} w\|_{\mathcal{X}} + \theta_1^2 \, \theta_2 \, \kappa_{\max} \, e^{\lambda T} \sum_{\boldsymbol{0}\ne\boldsymbol{m}<\boldsymbol{\nu}} \binom{\boldsymbol{\nu}}{\boldsymbol{m}} \|\partial_{\boldsymbol{y}}^{\boldsymbol{m}} w\|_{\mathcal{X}} \, \|\partial_{\boldsymbol{y}}^{\boldsymbol{\nu}-\boldsymbol{m}} w\|_{\mathcal{X}} \\
&\qquad + \theta_1^2 \, \theta_2 \, e^{\lambda T} \sum_{j\ge 1} \nu_j \, \beta_j \sum_{\boldsymbol{m}\le\boldsymbol{\nu}-\boldsymbol{e}_j} \binom{\boldsymbol{\nu}-\boldsymbol{e}_j}{\boldsymbol{m}} \|\partial_{\boldsymbol{y}}^{\boldsymbol{m}} w\|_{\mathcal{X}} \, \|\partial_{\boldsymbol{y}}^{\boldsymbol{\nu}-\boldsymbol{e}_j-\boldsymbol{m}} w\|_{\mathcal{X}} \; =: \; \Theta_{\boldsymbol{\nu}}. \qquad (3.14)
\end{aligned}
$$

TIME DERIVATIVE. We return to (3.10) but remove the integration over $t \in I$. For a.e. $t \in I$ we have

$$
\begin{aligned}
&\int_\Omega \frac{\partial}{\partial t}(\partial_{\boldsymbol{y}}^{\boldsymbol{\nu}} w) \, v \, \mathrm{d}\boldsymbol{x} + \int_\Omega a \, \nabla(\partial_{\boldsymbol{y}}^{\boldsymbol{\nu}} w) \cdot \nabla v \, \mathrm{d}\boldsymbol{x} + \int_\Omega 2 \, b \, (\partial_{\boldsymbol{y}}^{\boldsymbol{\nu}} w) \, w \, v \, \mathrm{d}\boldsymbol{x} + \int_\Omega c \, (\partial_{\boldsymbol{y}}^{\boldsymbol{\nu}} w) \, v \, \mathrm{d}\boldsymbol{x} \\
&= - \sum_{j\ge 1} \nu_j \int_\Omega \psi_j \, \nabla(\partial_{\boldsymbol{y}}^{\boldsymbol{\nu}-\boldsymbol{e}_j} w) \cdot \nabla v \, \mathrm{d}\boldsymbol{x} + \sum_{j\ge 1} \nu_j \int_\Omega \xi_j \, (\partial_{\boldsymbol{y}}^{\boldsymbol{\nu}-\boldsymbol{e}_j} w) \, v \, \mathrm{d}\boldsymbol{x} \\
&\quad - \sum_{\boldsymbol{0}\ne\boldsymbol{m}<\boldsymbol{\nu}} \binom{\boldsymbol{\nu}}{\boldsymbol{m}} \int_\Omega b \, (\partial_{\boldsymbol{y}}^{\boldsymbol{m}} w) \, (\partial_{\boldsymbol{y}}^{\boldsymbol{\nu}-\boldsymbol{m}} w) \, v \, \mathrm{d}\boldsymbol{x} \\
&\quad - \sum_{j\ge 1} \nu_j \sum_{\boldsymbol{m}\le\boldsymbol{\nu}-\boldsymbol{e}_j} \binom{\boldsymbol{\nu}-\boldsymbol{e}_j}{\boldsymbol{m}} \int_\Omega \xi_j \, e^{\lambda t} \, (\partial_{\boldsymbol{y}}^{\boldsymbol{m}} w) \, (\partial_{\boldsymbol{y}}^{\boldsymbol{\nu}-\boldsymbol{e}_j-\boldsymbol{m}} w) \, v \, \mathrm{d}\boldsymbol{x}.
\end{aligned}
$$

Using $0 \le w \le e^{-\lambda t}$ to obtain $|2 \, b \, (\partial_{\boldsymbol{y}}^{\boldsymbol{\nu}} w) \, w \, v + c \, (\partial_{\boldsymbol{y}}^{\boldsymbol{\nu}} w) \, v| \le |\kappa + \lambda + f| \, |\partial_{\boldsymbol{y}}^{\boldsymbol{\nu}} w| \, |v|$, and applying the Cauchy–Schwarz and Hölder inequalities, we obtain

$$
\begin{aligned}
&\Big| \int_\Omega \frac{\partial}{\partial t}(\partial_{\boldsymbol{y}}^{\boldsymbol{\nu}} w) \, v \, \mathrm{d}\boldsymbol{x} \Big| \\
&\le a_{\max} \, \|\nabla(\partial_{\boldsymbol{y}}^{\boldsymbol{\nu}} w)(\cdot,t)\|_{L^2(\Omega)} \, \|\nabla v\|_{L^2(\Omega)} + (\kappa_{\max} + \lambda + f_{\max}) \, \|\partial_{\boldsymbol{y}}^{\boldsymbol{\nu}} w(\cdot,t)\|_{L^2(\Omega)} \, \|v\|_{L^2(\Omega)} \\
&\quad + \sum_{j\ge 1} \nu_j \, \beta_j \, \|\nabla(\partial_{\boldsymbol{y}}^{\boldsymbol{\nu}-\boldsymbol{e}_j} w)(\cdot,t)\|_{L^2(\Omega)} \, \|\nabla v\|_{L^2(\Omega)} + \sum_{j\ge 1} \nu_j \, \beta_j \, \|\partial_{\boldsymbol{y}}^{\boldsymbol{\nu}-\boldsymbol{e}_j} w(\cdot,t)\|_{L^2(\Omega)} \, \|v\|_{L^2(\Omega)} \\
&\quad + \kappa_{\max} \, e^{\lambda T} \sum_{\boldsymbol{0}\ne\boldsymbol{m}<\boldsymbol{\nu}} \binom{\boldsymbol{\nu}}{\boldsymbol{m}} \|\partial_{\boldsymbol{y}}^{\boldsymbol{m}} w(\cdot,t)\|_{L^2(\Omega)} \, \|\partial_{\boldsymbol{y}}^{\boldsymbol{\nu}-\boldsymbol{m}} w(\cdot,t)\|_{L^4(\Omega)} \, \|v\|_{L^4(\Omega)} \\
&\quad + e^{\lambda T} \sum_{j\ge 1} \nu_j \, \beta_j \sum_{\boldsymbol{m}\le\boldsymbol{\nu}-\boldsymbol{e}_j} \binom{\boldsymbol{\nu}-\boldsymbol{e}_j}{\boldsymbol{m}} \|\partial_{\boldsymbol{y}}^{\boldsymbol{m}} w(\cdot,t)\|_{L^2(\Omega)} \, \|\partial_{\boldsymbol{y}}^{\boldsymbol{\nu}-\boldsymbol{e}_j-\boldsymbol{m}} w(\cdot,t)\|_{L^4(\Omega)} \, \|v\|_{L^4(\Omega)}.
\end{aligned}
$$

Using $\|\nabla v\|_{L^2(\Omega)} \le \|v\|_{H^1(\Omega)}$ and $\|v\|_{L^4(\Omega)} \le \theta_1 \, \|v\|_{H^1(\Omega)}$, the last factor of every term on the right-hand side can be bounded in terms of $\|v\|_{H^1(\Omega)}$. Therefore we conclude that

$$
\begin{aligned}
&\|\tfrac{\partial}{\partial t}(\partial_{\boldsymbol{y}}^{\boldsymbol{\nu}} w)(\cdot,t)\|_{H^1(\Omega)^*} \\
&\le (a_{\max} + \kappa_{\max} + \lambda + f_{\max}) \, \|\partial_{\boldsymbol{y}}^{\boldsymbol{\nu}} w(\cdot,t)\|_{H^1(\Omega)} + 2 \sum_{j\ge 1} \nu_j \, \beta_j \, \|\partial_{\boldsymbol{y}}^{\boldsymbol{\nu}-\boldsymbol{e}_j} w(\cdot,t)\|_{H^1(\Omega)} \\
&\quad + \theta_1^2 \, \theta_2 \, \kappa_{\max} \, e^{\lambda T} \sum_{\boldsymbol{0}\ne\boldsymbol{m}<\boldsymbol{\nu}} \binom{\boldsymbol{\nu}}{\boldsymbol{m}} \|\partial_{\boldsymbol{y}}^{\boldsymbol{m}} w\|_{\mathcal{X}} \, \|\partial_{\boldsymbol{y}}^{\boldsymbol{\nu}-\boldsymbol{m}} w(\cdot,t)\|_{H^1(\Omega)} \\
&\quad + \theta_1^2 \, \theta_2 \, e^{\lambda T} \sum_{j\ge 1} \nu_j \, \beta_j \sum_{\boldsymbol{m}\le\boldsymbol{\nu}-\boldsymbol{e}_j} \binom{\boldsymbol{\nu}-\boldsymbol{e}_j}{\boldsymbol{m}} \|\partial_{\boldsymbol{y}}^{\boldsymbol{m}} w\|_{\mathcal{X}} \, \|\partial_{\boldsymbol{y}}^{\boldsymbol{\nu}-\boldsymbol{e}_j-\boldsymbol{m}} w(\cdot,t)\|_{H^1(\Omega)}, \qquad (3.15)
\end{aligned}
$$

where we also used $\|\partial_{\boldsymbol{y}}^{\boldsymbol{m}} w(\cdot,t)\|_{L^2(\Omega)} \le \|\partial_{\boldsymbol{y}}^{\boldsymbol{m}} w\|_{C(I;L^2(\Omega))} \le \theta_2 \, \|\partial_{\boldsymbol{y}}^{\boldsymbol{m}} w\|_{\mathcal{X}}$. This step to remove the dependence of one factor on t is crucial before we integrate over $t \in I$.

Next we square both sides of (3.15), integrate over $t \in I$, and then take the square root. We can view the entire right-hand side of (3.15) as a sum of the form $\sum_k \alpha_k\, g_k(t)$, and so we use the estimate

$$\begin{aligned}
\bigg(\int_I \Big(\sum_k \alpha_k\, g_k(t)\Big)^2 \,\mathrm{d}t\bigg)^{1/2} &= \bigg(\sum_k \sum_{k'} \alpha_k\, \alpha_{k'} \int_I g_k(t)\, g_{k'}(t)\,\mathrm{d}t\bigg)^{1/2} \\
&\le \bigg(\sum_k \sum_{k'} \alpha_k\, \alpha_{k'} \Big(\int_I g_k^2(t)\,\mathrm{d}t\Big)^{1/2} \Big(\int_I g_{k'}^2(t)\,\mathrm{d}t\Big)^{1/2}\bigg)^{1/2} \\
&= \sum_k \alpha_k \Big(\int_I g_k^2(t)\,\mathrm{d}t\Big)^{1/2}.
\end{aligned}$$

This leads to

$$\begin{aligned}
&\|\tfrac{\partial}{\partial t}(\partial_{\boldsymbol{y}}^{\boldsymbol{\nu}} w)\|_{L^2(I;H^1(\Omega)^*)} \\
&\le (a_{\max} + \kappa_{\max} + \lambda + f_{\max})\, \|\partial_{\boldsymbol{y}}^{\boldsymbol{\nu}} w\|_{L^2(I;H^1(\Omega))} + 2 \sum_{j\ge1} \nu_j\, \beta_j\, \|\partial_{\boldsymbol{y}}^{\boldsymbol{\nu}-\boldsymbol{e}_j} w\|_{L^2(I;H^1(\Omega))} \\
&\quad + \theta_1^2\, \theta_2\, \kappa_{\max}\, e^{\lambda T} \sum_{\boldsymbol{0}\ne\boldsymbol{m}<\boldsymbol{\nu}} \binom{\boldsymbol{\nu}}{\boldsymbol{m}} \|\partial_{\boldsymbol{y}}^{\boldsymbol{m}} w\|_{\mathcal{X}}\, \|\partial_{\boldsymbol{y}}^{\boldsymbol{\nu}-\boldsymbol{m}} w\|_{L^2(I;H^1(\Omega))} \\
&\quad + \theta_1^2\, \theta_2\, e^{\lambda T} \sum_{j\ge1} \nu_j\, \beta_j \sum_{\boldsymbol{m}\le\boldsymbol{\nu}-\boldsymbol{e}_j} \binom{\boldsymbol{\nu}-\boldsymbol{e}_j}{\boldsymbol{m}} \|\partial_{\boldsymbol{y}}^{\boldsymbol{m}} w\|_{\mathcal{X}}\, \|\partial_{\boldsymbol{y}}^{\boldsymbol{\nu}-\boldsymbol{e}_j-\boldsymbol{m}} w\|_{L^2(I;H^1(\Omega))} \\
&\le (a_{\max} + \kappa_{\max} + \lambda + f_{\max})\, \|\partial_{\boldsymbol{y}}^{\boldsymbol{\nu}} w\|_{L^2(I;H^1(\Omega))} + \Theta_{\boldsymbol{\nu}},
\end{aligned} \tag{3.16}$$

where $\Theta_{\boldsymbol{\nu}}$ is precisely the right-hand side of (3.14).

Recursion. Using (3.14) and (3.16), we obtain

$$\begin{aligned}
\|\partial_{\boldsymbol{y}}^{\boldsymbol{\nu}} w\|_{\mathcal{X}} &= \sqrt{\|\partial_{\boldsymbol{y}}^{\boldsymbol{\nu}} w\|^2_{L^2(I;H^1(\Omega))} + \|\tfrac{\partial}{\partial t}(\partial_{\boldsymbol{y}}^{\boldsymbol{\nu}} w)\|^2_{L^2(I;H^1(\Omega)^*)}} \\
&\le \|\partial_{\boldsymbol{y}}^{\boldsymbol{\nu}} w\|_{L^2(I;H^1(\Omega))} + \|\tfrac{\partial}{\partial t}(\partial_{\boldsymbol{y}}^{\boldsymbol{\nu}} w)\|_{L^2(I;H^1(\Omega)^*)} \\
&\le (1 + a_{\max} + \kappa_{\max} + \lambda + f_{\max})\, \|\partial_{\boldsymbol{y}}^{\boldsymbol{\nu}} w\|_{L^2(I;H^1(\Omega))} + \Theta_{\boldsymbol{\nu}} \\
&\le (1 + a_{\max} + \kappa_{\max} + \lambda + f_{\max})\, \frac{\Theta_{\boldsymbol{\nu}}}{\min(a_{\min}, \lambda - \kappa_{\max})} + \Theta_{\boldsymbol{\nu}},
\end{aligned}$$

which yields the recursion

$$\begin{aligned}
\|\partial_{\boldsymbol{y}}^{\boldsymbol{\nu}} w\|_{\mathcal{X}} \le \Phi \bigg[& 2 \sum_{j\ge1} \nu_j\, \beta_j\, \|\partial_{\boldsymbol{y}}^{\boldsymbol{\nu}-\boldsymbol{e}_j} w\|_{\mathcal{X}} + \theta_1^2\, \theta_2\, \kappa_{\max}\, e^{\lambda T} \sum_{\boldsymbol{0}\ne\boldsymbol{m}<\boldsymbol{\nu}} \binom{\boldsymbol{\nu}}{\boldsymbol{m}} \|\partial_{\boldsymbol{y}}^{\boldsymbol{m}} w\|_{\mathcal{X}}\, \|\partial_{\boldsymbol{y}}^{\boldsymbol{\nu}-\boldsymbol{m}} w\|_{\mathcal{X}} \\
& + \theta_1^2\, \theta_2\, e^{\lambda T} \sum_{j\ge1} \nu_j\, \beta_j \sum_{\boldsymbol{m}\le\boldsymbol{\nu}-\boldsymbol{e}_j} \binom{\boldsymbol{\nu}-\boldsymbol{e}_j}{\boldsymbol{m}} \|\partial_{\boldsymbol{y}}^{\boldsymbol{m}} w\|_{\mathcal{X}}\, \|\partial_{\boldsymbol{y}}^{\boldsymbol{\nu}-\boldsymbol{e}_j-\boldsymbol{m}} w\|_{\mathcal{X}} \bigg],
\end{aligned} \tag{3.17}$$

where we abbreviated

$$\Phi := \frac{1 + a_{\max} + \kappa_{\max} + \lambda + f_{\max}}{\min(a_{\min}, \lambda - \kappa_{\max})} + 1. \tag{3.18}$$

Induction. We will prove by induction on $|\boldsymbol{\nu}|$ that

$$\|\partial_{\boldsymbol{y}}^{\boldsymbol{\nu}} w\|_{\mathcal{X}} \le D\, \boldsymbol{\beta}^{\boldsymbol{\nu}} \rho^{|\boldsymbol{\nu}|-1} \left[\tfrac{1}{2}\right]_{|\boldsymbol{\nu}|} \qquad \text{for all } \boldsymbol{\nu} \ne \boldsymbol{0}, \tag{3.19}$$

with constants D and ρ to be specified below.

Our base step is $|\boldsymbol{\nu}| = 1$ (rather than $\boldsymbol{\nu} = \mathbf{0}$, as in typical regularity proofs) because our recursion (3.17) involves a sum over $\mathbf{0} \neq \boldsymbol{m} < \boldsymbol{\nu}$ which is empty if $|\boldsymbol{\nu}| = 1$. Recall from Theorem 2.2 that we have the a priori bound $\|w\|_{\mathcal{X}} \le C\,\|w_0\|_{L^2(\Omega)}$, where $\|w_0\|_{L^2(\Omega)} \le 1$ since $0 \le w_0(\boldsymbol{x}) \le 1$. For $\boldsymbol{\nu} = \boldsymbol{e}_k$ for some $k \ge 1$, the recursion (3.17) gives

$$\begin{aligned}\|\partial_{\boldsymbol{y}}^{\boldsymbol{e}_k} w\|_{\mathcal{X}} &\le \Phi\left(2\,\beta_k\,\|w\|_{\mathcal{X}} + \theta_1^2\,\theta_2\,e^{\lambda T}\,\beta_k\,\|w\|_{\mathcal{X}}^2\right)\\ &\le \Phi\left(2\,\beta_k\,C\,\|w_0\|_{L^2(\Omega)} + \theta_1^2\,\theta_2\,e^{\lambda T}\,\beta_k\,C^2\,\|w_0\|_{L^2(\Omega)}^2\right) \le \frac{D\,\beta_k}{2},\end{aligned}$$

as required in (3.19), if we define

$$D := 2\,\Phi\,C\left(2 + C\,\theta_1^2\,\theta_2\,e^{\lambda T}\right)\|w_0\|_{L^2(\Omega)} \le 2\,\Phi\,C\left(2 + C\,\theta_1^2\,\theta_2\,e^{\lambda T}\right) =: E. \tag{3.20}$$

For the induction step, let $|\boldsymbol{\nu}| \ge 2$ and suppose (3.19) is true for all multiindices of order less than $|\boldsymbol{\nu}|$. We have from (3.17)

$$\begin{aligned}&(1/\Phi)\,\|\partial_{\boldsymbol{y}}^{\boldsymbol{\nu}} w\|_{\mathcal{X}}\\ &\le 2\sum_{j\ge1}\nu_j\,\beta_j\,D\,\boldsymbol{\beta}^{\boldsymbol{\nu}-\boldsymbol{e}_j}\rho^{|\boldsymbol{\nu}-\boldsymbol{e}_j|-1}\,[\tfrac12]_{|\boldsymbol{\nu}-\boldsymbol{e}_j|}\\ &\quad+\theta_1^2\,\theta_2\,\kappa_{\max}\,e^{\lambda T}\sum_{\mathbf{0}\neq\boldsymbol{m}<\boldsymbol{\nu}}\binom{\boldsymbol{\nu}}{\boldsymbol{m}}D\,\boldsymbol{\beta}^{\boldsymbol{m}}\rho^{|\boldsymbol{m}|-1}\,[\tfrac12]_{|\boldsymbol{m}|}\,D\,\boldsymbol{\beta}^{\boldsymbol{\nu}-\boldsymbol{m}}\rho^{|\boldsymbol{\nu}-\boldsymbol{m}|-1}\,[\tfrac12]_{|\boldsymbol{\nu}-\boldsymbol{m}|}\\ &\quad+\theta_1^2\,\theta_2\,e^{\lambda T}\sum_{j\ge1}\nu_j\,\beta_j\sum_{\boldsymbol{m}\le\boldsymbol{\nu}-\boldsymbol{e}_j}\binom{\boldsymbol{\nu}-\boldsymbol{e}_j}{\boldsymbol{m}}D\,\boldsymbol{\beta}^{\boldsymbol{m}}\rho^{|\boldsymbol{m}|-1}\,[\tfrac12]_{|\boldsymbol{m}|}\,D\,\boldsymbol{\beta}^{\boldsymbol{\nu}-\boldsymbol{e}_j-\boldsymbol{m}}\rho^{|\boldsymbol{\nu}-\boldsymbol{e}_j-\boldsymbol{m}|-1}\,[\tfrac12]_{|\boldsymbol{\nu}-\boldsymbol{e}_j-\boldsymbol{m}|}\\ &\le 2\,D\,\boldsymbol{\beta}^{\boldsymbol{\nu}}\rho^{|\boldsymbol{\nu}|-2}\,|\boldsymbol{\nu}|\,[\tfrac12]_{|\boldsymbol{\nu}|-1} + D^2\theta_1^2\,\theta_2\,\kappa_{\max}\,e^{\lambda T}\,\boldsymbol{\beta}^{\boldsymbol{\nu}}\rho^{|\boldsymbol{\nu}|-2}\sum_{\mathbf{0}\neq\boldsymbol{m}<\boldsymbol{\nu}}\binom{\boldsymbol{\nu}}{\boldsymbol{m}}[\tfrac12]_{|\boldsymbol{m}|}\,[\tfrac12]_{|\boldsymbol{\nu}-\boldsymbol{m}|}\\ &\quad+D^2\theta_1^2\,\theta_2\,e^{\lambda T}\boldsymbol{\beta}^{\boldsymbol{\nu}}\rho^{|\boldsymbol{\nu}|-3}\sum_{j\ge1}\nu_j\sum_{\boldsymbol{m}\le\boldsymbol{\nu}-\boldsymbol{e}_j}\binom{\boldsymbol{\nu}-\boldsymbol{e}_j}{\boldsymbol{m}}[\tfrac12]_{|\boldsymbol{m}|}\,[\tfrac12]_{|\boldsymbol{\nu}-\boldsymbol{e}_j-\boldsymbol{m}|}.\end{aligned}$$

Using (3.5), this leads to

$$\begin{aligned}(1/\Phi)\,\|\partial_{\boldsymbol{y}}^{\boldsymbol{\nu}} w\|_{\mathcal{X}} &\le 2\,D\,\boldsymbol{\beta}^{\boldsymbol{\nu}}\rho^{|\boldsymbol{\nu}|-2}\,|\boldsymbol{\nu}|\,[\tfrac12]_{|\boldsymbol{\nu}|-1} + D^2\theta_1^2\,\theta_2\,\kappa_{\max}\,e^{\lambda T}\,\boldsymbol{\beta}^{\boldsymbol{\nu}}\rho^{|\boldsymbol{\nu}|-2}\cdot 2\,[\tfrac12]_{|\boldsymbol{\nu}|}\\ &\quad+D^2\theta_1^2\,\theta_2\,e^{\lambda T}\boldsymbol{\beta}^{\boldsymbol{\nu}}\rho^{|\boldsymbol{\nu}|-3}\,|\boldsymbol{\nu}|\cdot\left(2\,[\tfrac12]_{|\boldsymbol{\nu}|-1} + 2\,[\tfrac12]_{|\boldsymbol{\nu}|-1}\right)\\ &\le D\,\boldsymbol{\beta}^{\boldsymbol{\nu}}\rho^{|\boldsymbol{\nu}|-2}\,[\tfrac12]_{|\boldsymbol{\nu}|}\left(8 + 2E\,\theta_1^2\,\theta_2\,\kappa_{\max}\,e^{\lambda T} + 16E\,\theta_1^2\,\theta_2\,e^{\lambda T}\right),\end{aligned}$$

where assumed $\rho \ge 1$ so that $\rho^{|\boldsymbol{\nu}|-3} \le \rho^{|\boldsymbol{\nu}|-2}$, and used $D^2 \le DE$ (see (3.20)), together with

$$n\,[\tfrac12]_{n-1} = \frac{n}{|\frac12 - n + 1|}\,[\tfrac12]_n \le \frac{n}{\frac14 n}\,[\tfrac12]_n = 4\,[\tfrac12]_n \quad \text{for all } n \ge 2.$$

Defining

$$\rho := 2\,\Phi\left(4 + E\,\theta_1^2\,\theta_2\,(\kappa_{\max} + 8)\,e^{\lambda T}\right) \ge 1, \tag{3.21}$$

we arrive at the required bound (3.19). This completes the induction proof.

We have written the hypothesis (3.19) in a convenient form for induction, where the factor ρ served as a scaling parameter that can be adjusted to suit our needs, as we defined in (3.21). Since $D = E\,\|w_0\|_{L^2(\Omega)}$ (see (3.20)), this factor ρ can be seen as a rescaling of the sequence β_j as follows:

$$\|\partial_{\boldsymbol{y}}^{\boldsymbol{\nu}} w\|_{\mathcal{X}} \le D\,\boldsymbol{\beta}^{\boldsymbol{\nu}}\rho^{|\boldsymbol{\nu}|-1}\,[\tfrac12]_{|\boldsymbol{\nu}|} = \tfrac{D}{\rho}\,(\rho\,\boldsymbol{\beta})^{\boldsymbol{\nu}}\,[\tfrac12]_{|\boldsymbol{\nu}|} = \tfrac{E}{\rho}\,(\rho\,\boldsymbol{\beta})^{\boldsymbol{\nu}}\,[\tfrac12]_{|\boldsymbol{\nu}|}\,\|w_0\|_{L^2(\Omega)} \quad \text{for all } \boldsymbol{\nu} \neq \mathbf{0}.$$

The result can be extended to cover also the $\boldsymbol{\nu} = \mathbf{0}$ case as follows

$$\|\partial_{\boldsymbol{y}}^{\boldsymbol{\nu}} w\|_{\mathcal{X}} \le \max(C, \tfrac{E}{\rho})\,(\rho\,\boldsymbol{\beta})^{\boldsymbol{\nu}}\,[\tfrac12]_{|\boldsymbol{\nu}|}\,\|w_0\|_{L^2(\Omega)} \quad \text{for all } \boldsymbol{\nu}.$$

Finally, since $u = e^{\lambda t}\,w$, we can follow the last step in the proof of Theorem 2.2 to obtain $\|\partial_{\boldsymbol{y}}^{\boldsymbol{\nu}} u\|_{\mathcal{X}} \le \sqrt{\max(1+2\lambda^2, 2)}\,e^{\lambda T}\,\|\partial_{\boldsymbol{y}}^{\boldsymbol{\nu}} w\|_{\mathcal{X}}$. □

4 QMC error analysis for uniform random fields

We now fix $\psi_j \equiv 0$ for j even and $\xi_j \equiv 0$ for j odd to make the two fields independent. We truncate the random fields to s terms and denote the corresponding PDE solution by $u_s^{\boldsymbol{y}}$ with $\boldsymbol{y} = (y_1, \ldots, y_s, 0, \ldots)$. We are interested in the expected value of the solution u_s with respect to the random parameter $\boldsymbol{y} \in U_s := [-\frac{1}{2}, \frac{1}{2}]^s$,

$$\mathbb{E}[u_s] := \int_{U_s} u_s^{\boldsymbol{y}} \,\mathrm{d}\boldsymbol{y}.$$

We approximate this integral using a randomly shifted lattice rule with generating vector $\boldsymbol{z} \in \mathbb{Z}^s$ and uniformly generated random shift $\boldsymbol{\Delta} \in [0,1]^s$,

$$Q_N(u_s) := \frac{1}{N} \sum_{i=1}^{N} u^{\boldsymbol{y}_{\boldsymbol{\Delta}}^{(i)}}, \quad \text{with} \quad \boldsymbol{y}_{\boldsymbol{\Delta}}^{(i)} := (\tfrac{i}{N}\,\boldsymbol{z} + \boldsymbol{\Delta}) \bmod 1 - \tfrac{\mathbf{1}}{\mathbf{2}}, \tag{4.1}$$

where the subtraction by $\frac{\mathbf{1}}{\mathbf{2}} = (\frac{1}{2}, \ldots, \frac{1}{2})$ translates points from the standard unit cube $[0,1]^s$ to U_s. Alternatively, we may wish to compute the expectation of a QoI given by a bounded linear functional G of the PDE solution $u_s^{\boldsymbol{y}}$, in which case we approximate $\mathbb{E}[G(u_s)] \approx Q_N(G(u_s^{\boldsymbol{y}}))$, with the QMC rule applied analogously as in (4.1). For now we work with the exact PDE solution (i.e., no finite element method or time discretization).

Using the parametric regularity bound established in Theorem 3.1, we can apply two general theorems from [21] for Banach-space-valued functions depending on affine uniform parameters $\boldsymbol{y}$, to obtain a dimension truncation error bound and a QMC error bound. We analyze the QMC error in the first-order weighted unanchored Sobolev space with weight parameters $\boldsymbol{\gamma} := (\gamma_{\mathfrak{u}})_{\mathfrak{u} \subset \mathbb{N}}$, see e.g., [29].

Theorem 4.1 (dimension truncation error) *Suppose that $\|\psi_1\|_\infty \geq \|\psi_3\|_\infty \geq \|\psi_5\|_\infty \geq \cdots$ and $\|\xi_2\|_\infty \geq \|\xi_4\|_\infty \geq \|\xi_6\|_\infty \geq \cdots$, and $\sum_{j\geq 1} \beta_j^p = \sum_{j \geq 1} \max(\|\psi_j\|_\infty, \|\xi_j\|_\infty)^p < \infty$ for some $p \in (0,1)$. Then for all $s \in \mathbb{N}$ the dimension truncation error satisfies*

$$\big\|\, \mathbb{E}[u - u_s] \,\big\|_{\mathcal{X}} = \Big\| \int_U (u^{\boldsymbol{y}} - u^{\boldsymbol{y}_s}) \,\mathrm{d}\boldsymbol{y} \Big\|_{\mathcal{X}} = \widetilde{C}\, \|u_0\|_{L^2(\Omega)}\, C^*\, s^{-2/p+1},$$

where $\widetilde{C}$ is from Theorem 3.1 and $C^* > 0$ is independent of s.

Proof. Noting that $[\frac{1}{2}]_{|\boldsymbol{\nu}|} \leq |\boldsymbol{\nu}|!$, we apply [21, Theorem 6.2] by setting there $C_0 = \widetilde{C}\, \|u_0\|_{L^2(\Omega)}$, $r_1 = 0$, $r_2 = \rho$, and $\boldsymbol{\rho} = \boldsymbol{\beta}$. Our interleaved sequence $\boldsymbol{\beta}$ here is not strictly ordered as required in [21, Theorem 6.2], but the same result holds with a simple modification of the proof by splitting tail sums into separate and ordered sums of odd and even terms. □

Theorem 4.2 (QMC error bound) *We have the root-mean-square error bound with respect to the random shift*

$$\sqrt{\mathbb{E}_{\boldsymbol{\Delta}} \left[\big\|\mathbb{E}[u_s] - Q_N(u_s)\big\|_{\mathcal{X}}^2 \right]} \leq C_{s,\boldsymbol{\gamma},\lambda}\, [\phi_{\mathrm{tot}}(N)]^{-1/(2\lambda)} \quad \textit{for all } \lambda \in (\tfrac{1}{2}, 1],$$

or for any bounded linear functional $G : \mathcal{X} \to \mathbb{R}$,

$$\sqrt{\mathbb{E}_{\boldsymbol{\Delta}} \left[\big|\mathbb{E}[G(u_s)] - Q_N(G(u_s))\big|^2 \right]} \leq \|G\|_{\mathcal{X}^*}\, C_{s,\boldsymbol{\gamma},\lambda}\, [\phi_{\mathrm{tot}}(N)]^{-1/(2\lambda)} \quad \textit{for all } \lambda \in (\tfrac{1}{2}, 1],$$

where $\phi_{\mathrm{tot}}(N) := |\{1 \leq z \leq N-1 : \gcd(z,N) = 1\}|$ is the Euler totient function, with $1/\phi_{\mathrm{tot}}(N) \leq 2/N$ when N is a prime power, and

$$C_{s,\boldsymbol{\gamma},\lambda} := \widetilde{C} \bigg(\sum_{\emptyset \neq \mathfrak{u} \subseteq \{1:s\}} \gamma_{\mathfrak{u}}^\lambda \Big(\frac{2\,\zeta(2\lambda)}{(2\pi^2)^\lambda} \Big)^{|\mathfrak{u}|} \bigg)^{1/(2\lambda)} \bigg(\sum_{\mathfrak{u} \subseteq \{1:s\}} \frac{[\frac{1}{2}]_{|\mathfrak{u}|}^2 \prod_{j \in \mathfrak{u}} (\rho\, \beta_j)^2}{\gamma_{\mathfrak{u}}} \bigg)^{1/2},$$

where $\widetilde{C}$ *is defined in Theorem 3.1 and* ρ *is defined in* (3.21).

For some $p \in (0,1)$ *suppose that* $\sum_{j\geq 1} \beta_j^p = \sum_{j\geq 1} \max(\|\psi_j\|_\infty, \|\xi_j\|_\infty)^p < \infty$. *Then the best convergence rate* $\mathcal{O}(N^{-\min(1-\delta,\,1/p-1/2)})$ *is obtained by the following choices*

$$\lambda := \begin{cases} \frac{1}{2-2\delta} \text{ for all } \delta \in (0,1) & \text{if } p \in [0, \frac{2}{3}], \\ \frac{p}{2-p} & \text{if } p \in (\frac{2}{3}, 1), \end{cases} \qquad \gamma_{\mathfrak{u}} := \left([\tfrac{1}{2}]_{|\mathfrak{u}|} \prod_{j\in\mathfrak{u}} \frac{\rho\,\beta_j}{\sqrt{2\zeta(2\lambda)/(2\pi^2)^\lambda}} \right)^{2/(1+\lambda)}.$$

and the constant $C_{s,\gamma,\lambda}$ *is bounded independently of* s.

Proof. First we adapt [21, Theorem 6.6], with $|\mathfrak{u}|!$ replaced by $[\frac{1}{2}]_{|\mathfrak{u}|}$ and setting $C_0 = \widetilde{C}\,\|u_0\|_{L^2(\Omega)}$, $r_1 = 0$, $r_2 = \rho$, $\rho_j = \beta_j$, to obtain the root-mean-square error bounds. Then we follow [21, Theorem 6.8] to choose the parameter λ and the function space weights $\gamma_{\mathfrak{u}}$. □

5 Numerical experiments

5.1 Experiments with uniform random fields

We consider the spatial domain to be a square with length $L = L_{x_1} = L_{x_2} = 100\,\text{mm}$. The uncertain diffusion and reaction coefficients are defined as in (3.1)–(3.2), taken to be independent of t, i.e., stationary in time. The mean fields $a_0 := \psi_0(\boldsymbol{x}) = 0.05\ \text{mm}^2/\text{day}$ and $\kappa_0 := \xi_0(\boldsymbol{x}) = 0.3\ \text{day}^{-1}$ are taken to be in realistic ranges based on previous model calibration studies for gliomas [25]. The fluctuations are prescribed by interleaving two sequences as follow:

$$\psi_j(\boldsymbol{x}) = \begin{cases} a_0\, \frac{1}{2}\, k^{-\nu} \sin(\frac{k\,\pi\,x_1}{L_{x_1}})\, \sin(\frac{k\,\pi\,x_2}{L_{x_2}}) & \text{if } j = 2k-1. \\ 0 & \text{if } j = 2k, \end{cases}$$

$$\xi_j(\boldsymbol{x}) = \begin{cases} 0 & \text{if } j = 2k-1, \\ \kappa_0\, \frac{1}{2}\, k^{-\nu} \sin(\frac{k\,\pi\,x_1}{L_{x_1}})\, \sin(\frac{k\,\pi\,x_2}{L_{x_2}}) & \text{if } j = 2k, \end{cases}$$

for $j \geq 1$ with smoothness parameter $\nu = 2$.

The initial condition $u_0(\boldsymbol{x})$ is a Gaussian function in the center of the domain as in [40] and the terminal time is taken to be $T = 7$ days. Radiotherapy (2.3) is applied the first five days and chemotherapy (2.4) is administered daily. The radiotherapy dosage is uniformly $z_{\text{rt},k}(\boldsymbol{x}) = 2$ Gy and the chemotherapy concentration is assumed to be uniformly $z_{\text{ct},\ell}(\boldsymbol{x}) = 1$. The radiosensitivity parameter is $\alpha_{\text{rt}} = 0.025\,\text{Gy}^{-1}$ with ratio $\alpha_{\text{rt}}/\beta_{\text{rt}} = 10$ Gy following reported values in the literature [40]. The chemotherapy efficacy is $\alpha_{\text{ct}} = 0.9$ with clearance rate $\beta_{\text{ct}} = 24/1.8\ \text{day}^{-1}$. The implicit Euler method is used to discretize (2.1) in time with time step $\Delta t = 1/8$ day, such that $\gamma_{\text{rt},\varepsilon} = 1/\Delta t$. Linear finite elements are used to discretize the spatial dimension with mesh size $h = 1\,\text{mm}$.

We take the quantity of interest to be the total tumor cellularity at the end of the simulation horizon,

$$G(u_s^{\boldsymbol{y}}) := \int_\Omega u_s^{\boldsymbol{y}}(\boldsymbol{x}, T)\,\mathrm{d}\boldsymbol{x},$$

with stochastic dimension $s = 256$, that is, there are 128 terms in the expansion for each field. To obtain an unbiased estimator of $\mathbb{E}[G(u_s^{\boldsymbol{y}})]$, we average over R i.i.d. uniform random shifts,

$$\overline{Q} := \frac{1}{R}\sum_{r=1}^{R} Q_N^{(r)}(G(u_s)), \qquad Q_N^{(r)}[G(u_s)] := \frac{1}{N}\sum_{i=1}^{N} G\big(u^{\boldsymbol{y}^{(i)}_{\boldsymbol{\Delta}_r}}\big),$$

where, similarly to (4.1), $Q_N^{(r)}[G(u_s)]$ denotes the QMC approximation of the integral $\mathbb{E}[G(u_s)]$ with the rth random shift. To estimate the root-mean-square error in Theorem 4.2, we compute

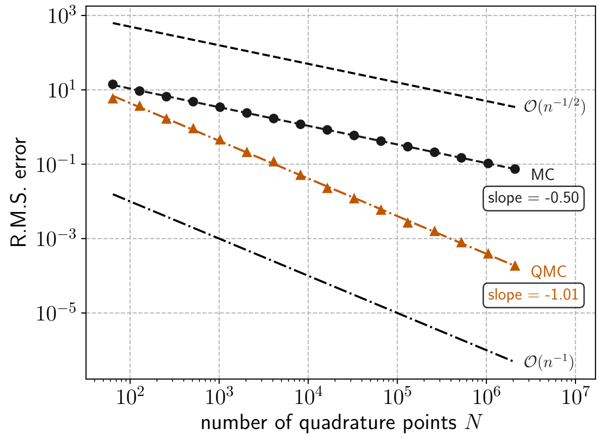

Figure 1: The approximate root-mean-square error (5.1) of the randomized QMC approximation and the standard error of the MC estimator of the integral $\mathbb{E}[G(u_s)]$ for different numbers of total PDE evaluations.

the approximation

$$\sqrt{\frac{1}{R(R-1)}\sum_{r=1}^{R}\left|\,\overline{Q}-Q_N^{(r)}(G(u_s))\,\right|^2}. \tag{5.1}$$

Here we use $R = 16$ random shifts $\boldsymbol{\Delta}$ and $N = 2^m$ lattice points with $m = [4, 5, \ldots, 17]$, for a total of $2^{21} = 2,097,152$ PDE evaluations. An off-the-shelf embedded lattice rule with weights tailored to a spectral decay rate of $1/j^2$ is utilized to generate the QMC sequence [11]. For comparison, we use $N^{\mathrm{MC}} = 2^{17} \cdot R = 2^{21}$ quadrature points for MC to match the total number of PDE evaluations. Computations are carried out on the Texas Advanced Computing Center's Frontera machine [41]. Code to reproduce the experiments is available at: https://github.com/gtpash/qmc-tumor. The results are displayed in Figure 1. We observe that the QMC root-mean-square error converges at a linear rate $\mathcal{O}(N^{-1})$ while standard MC converges with the typical $\mathcal{O}(N^{-1/2})$ rate, consistent with the theory.

5.2 Experiments with lognormal random fields

In this section, we consider a more realistic lognormal model for the uncertain coefficients, despite not yet having theoretical results as in the uniform case. The following lognormal model has been successfully employed in Bayesian inversion for gliomas in both murine models [30] and human patients [38],

$$a^{\boldsymbol{y}}(\boldsymbol{x}) = \psi_0(\boldsymbol{x}) + \exp(Z_a(\boldsymbol{x})),\ Z_a(\boldsymbol{x}) = \sum_{j=1}^{\infty} y_j\,\psi_j(\boldsymbol{x}),\ \psi_j = \begin{cases}\sqrt{\mu_{a,k}}\,\varphi_{a,k}(\boldsymbol{x}) & \text{if } j = 2k-1,\\ 0 & \text{if } j = 2k,\end{cases}$$

$$\kappa^{\boldsymbol{y}}(\boldsymbol{x}) = \xi_0(\boldsymbol{x}) + \exp(Z_\kappa(\boldsymbol{x})),\ Z_\kappa(\boldsymbol{x}) = \sum_{j=1}^{\infty} y_j\,\xi_j(\boldsymbol{x}),\ \ \xi_j = \begin{cases}0 & \text{if } j = 2k-1,\\ \sqrt{\mu_{\kappa,k}}\,\varphi_{\kappa,k}(\boldsymbol{x}) & \text{if } j = 2k,\end{cases}$$

with i.i.d. $y_j \sim \mathcal{N}(0,1)$. Here the parameters are stationary in time once more. The infinite sums are the Karhunen–Loève (KL) expansions [32] of the underlying Gaussian random fields $Z_a(\boldsymbol{x}) \sim \mathcal{N}(0, \mathcal{C}_a)$ and $Z_\kappa(\boldsymbol{x}) \sim \mathcal{N}(0, \mathcal{C}_\kappa)$ for the diffusion and proliferation coefficients, with ordered eigenpairs $\{(\mu_{a,k}, \varphi_{a,k})\}_k$ and $\{(\mu_{\kappa,k}, \varphi_{\kappa,k})\}_k$, respectively. We again interleave the two independent sequences. The foundational work of [31] established a link between Gaussian random fields with Matérn covariance operators and the solution of a stochastic PDE. Following

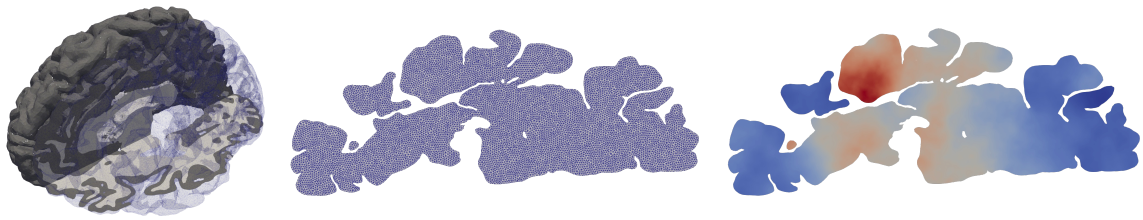

Figure 2: Left: Visualization of anatomy and slice of the left-hemisphere. Center: The computational mesh used for simulations, with 9,995 vertices. Right: A representative sample of the diffusion coefficient.

[42, 47], the covariance operators $\mathcal{C}_a$ and $\mathcal{C}_\kappa$ are taken to be the inverse of an elliptic operator of the form

$$\mathcal{C} := \mathcal{A}^{-\nu} = (-\gamma\,\Delta + \delta\, I)^{-\nu}, \tag{5.2}$$

with smoothness parameter $\nu = 2$ and hyperparameters $\gamma > 0$ and $\delta > 0$ that control the correlation length and pointwise variance [46]. We truncate the expansion and consider the s-dimensional subspace spanned by the leading eigenvectors. In particular, we solve a symmetrized (general) eigenvalue problem with a randomized double pass algorithm [47],

$$\mathbf{M}\,\mathbf{\Gamma}\,\boldsymbol{\varphi} = \mu\,\mathbf{M}\,\boldsymbol{\varphi}, \tag{5.3}$$

where $\mathbf{\Gamma} := \mathbf{R}^{-1}\mathbf{M}$ is the covariance matrix that arises from the discretization of (5.2), with mass matrix $\mathbf{M}_{ij} = \int_\Omega \phi_i(\boldsymbol{x})\phi_j(\boldsymbol{x})\,\mathrm{d}\boldsymbol{x}$ and bilinear form of the elliptic operator given by $\mathbf{R}_{ij} = \int_\Omega \phi_i(\boldsymbol{x})\mathcal{A}^\nu\phi_j(\boldsymbol{x})\,\mathrm{d}\boldsymbol{x}$. Here $\{\phi_i\}_{i=1}^m$ is the collection of finite element basis functions. The eigenpairs $\{(\mu_{a,k},\varphi_{a,k})\}_k$ and $\{(\mu_{\kappa,k},\varphi_{\kappa,k})\}_k$ obtained by solving (5.3) may be efficiently computed for generic unstructured domains.

In the numerical experiments, we fix the correlation length to 180 mm (roughly the largest dimension of a human brain). The pointwise variance is set to 0.2336 and 0.0682 for the diffusion and proliferation coefficients, respectively. As in Section 5.1, we take the mean fields to be $a_0 := \psi_0(\boldsymbol{x}) = 0.05$ mm^2/day and $\kappa_0 := \xi_0(\boldsymbol{x}) = 0.3$ day^{-1}. The domain is taken to be a two-dimensional slice of a human left-hemisphere [34]. The computational mesh is visualized along with a representative sample in Figure 2. The initial condition $u_0(\boldsymbol{x})$ is once more a Gaussian function centered at the geometric center of the domain with amplitude 0.8 and width 5.0 mm. The treatment schedule and radiosensitivity parameters are as in Section 5.1. A time step of $\Delta t = 1/8$ day is used for the temporal discretization and the unstructured mesh contains 9,995 vertices.

We empirically investigate the convergence rate using $R = 16$ random shifts $\mathbf{\Delta}$ and $N = 2^m$ lattice points with $m = [6, 7, \ldots 17]$. Each KL expansion is truncated at 512 terms, for a stochastic dimension of $s = 1024$. In the lognormal case, the shifted QMC points are $\boldsymbol{y}_{\mathbf{\Delta}}^{(i)} := \mathbf{\Phi}^{-1}\left(\left(\frac{i}{N}\,\boldsymbol{z} + \mathbf{\Delta}\right) \bmod 1\right)$, where $\mathbf{\Phi}^{-1}(\cdot)$ denotes the inverse cumulative normal distribution applied componentwise to a vector. The same embedded lattice rule as in the uniform case is used to construct the QMC sequence. The empirical spectrum of the covariance operators $\mathcal{C}_a$ and $\mathcal{C}_\kappa$ and convergence results are shown in Figure 3. We observe that the QMC root-mean-square error converges at a faster rate of $\mathcal{O}(N^{-0.87})$ than the MC rate of $\mathcal{O}(N^{-1/2})$. The square-root of the eigenvalues decay like $k^{-1.17}$ and so we expect the QMC convergence rate to be $1/p - 1/2 \approx 1.17 - 1/2 = 0.67$, if the theory for uniform fields also holds for lognormal fields (as proven for some elliptic linear problems). Hence our results are very encouraging and prompt further analysis.

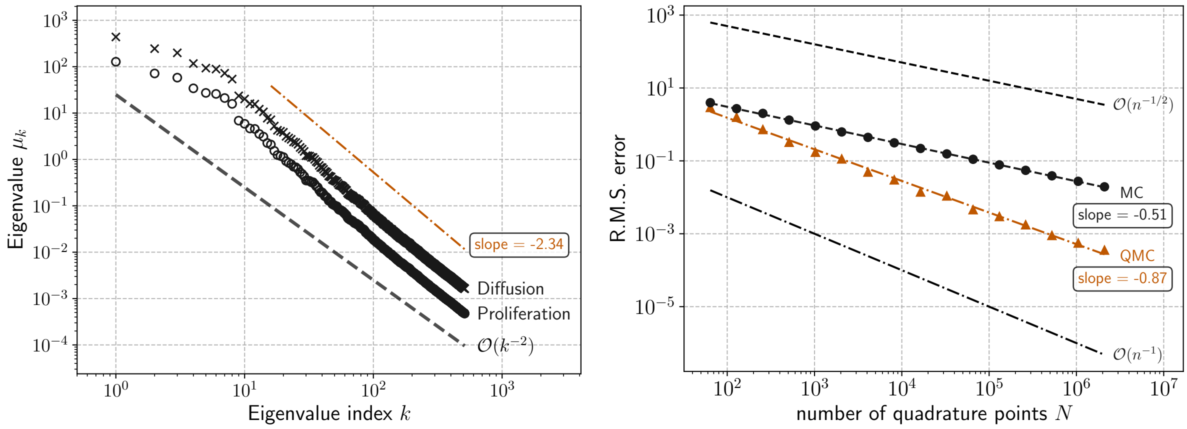

Figure 3: Left: The empirical spectral decay of the two Gaussian random fields compared to the theoretical rate accompanied. Right: The approximate root-mean-square error (5.1) for the QMC approximation and the standard error for the MC estimator of the integral $\mathbb{E}[G(u_s)]$.

6 Conclusions

In this work, we developed a QMC method for a semi-linear parabolic PDE model of tumor growth. The method was applied to the high-dimensional integral arising from estimating the expected value of a smooth QoI. We developed a well-posedness argument for this particular class of problems and derived an *a priori* bound with an explicit constant. Moreover, in the case of uniform random fields we obtained a parametric regularity bound to provide theoretical error bounds for the QMC approximation. The convergence rate was then numerically verified, in particular, we observe linear convergence. Additionally, we numerically studied application to lognormal random fields and once more observed faster than MC convergence. Future work will focus on extending approximation theory to the lognormal case and application to an optimal control problem. Furthermore, a rigorous analysis of the dimension truncation error as well as the numerical discretization of the PDE should be executed to assess their contributions to the overall discretization error.

Acknowledgments

The authors are grateful for insightful discussions with Albert Cohen, Wolfgang Dahmen, Mike Giles, Maria Pia Gualdani, Pierre L'Ecuyer, Dingcheng Luo, Fabio Nobile, Mark Peletier, William Porteous, and Christian Wieners, as well as other participants at the 2025 Oberwolfach Workshop on Computation and Learning in High Dimensions.

References

[1] J. Alfonso, K. Talkenberger, M. Seifert, B. Klink, A. Hawkins-Daarud, K. Swanson, H. Hatzikirou, and A. Deutsch, *The biology and mathematical modelling of glioma invasion: a review*, Journal of the Royal Society Interface, 14 (2017), p. 20170490.

[2] X. An, J. Dick, M. Feischl, A. Scaglioni, and T. Tran, *Sparse Grid Approximation of Nonlinear SPDEs: The Landau–Lifshitz–Gilbert Equation*, SIAM/ASA J. Uncertain. Quantif., 13 (2025), pp. 472–517.

[3] G. Borasi and A. Nahum, *Modelling the radiotherapy effect in the reaction-diffusion equation*, Physica Medica, 32 (2016), pp. 1175–1179.

[4] G. Cavalleri, P. Colli, A. Miranville, and E. Rocca, *On a brain tumor growth model with lactate metabolism, viscoelastic effects, and tissue damage*, Nonlinear Anal. Real World Appl., 87 (2026), p. 104419.

[5] M. Chaplain, *Avascular growth, angiogenesis and vascular growth in solid tumours: The mathematical modelling of the stages of tumour development*, Math. Comput. Model., 23 (1996), pp. 47–87.

[6] A. Chernov and T. Lê, *Analytic and Gevrey class regularity for parametric elliptic eigenvalue problems and applications*, SIAM J. Numer. Anal., 62 (2024), pp. 1874–1900.

[7] A. Chernov and T. Lê, *Analytic and Gevrey class regularity for parametric semilinear reaction-diffusion problems and applications in uncertainty quantification*, Comput. Math. Appl., 164 (2024), pp. 116–130.

[8] A. Chernov and T. Lê, *Gevrey class regularity for steady-state incompressible Navier-Stokes equations in parametric domains and related models*, arXiv preprint arXiv:2504.13753, (2025).

[9] O. Clatz, M. Sermesant, P.-Y. Bondiau, H. Delingette, S. K. Warfield, G. Malandain, and N. Ayache, *Realistic simulation of the 3-D growth of brain tumors in MR images coupling diffusion with biomechanical deformation*, IEEE Trans. Med. Imaging, 24 (2005), pp. 1334–1346.

[10] P. Colli, H. Gomez, G. Lorenzo, G. Marinoschi, A. Reali, and E. Rocca, *Mathematical analysis and simulation study of a phase-field model of prostate cancer growth with chemotherapy and antiangiogenic therapy effects*, Math. Models Methods Appl. Sci., 30 (2020), pp. 1253–1295.

[11] R. Cools, F. Y. Kuo, and D. Nuyens, *Constructing embedded lattice rules for multivariate integration*, SIAM J. Sci. Comput., 28 (2006), pp. 2162–2188.

[12] J. Dick, F. Y. Kuo, Q. T. Le Gia, D. Nuyens, and C. Schwab, *Higher order QMC Petrov–Galerkin discretization for affine parametric operator equations with random field inputs*, SIAM J. Numer. Anal., 52 (2014), pp. 2676–2702.

[13] L. C. Evans, *Partial Differential Equations*, vol. 19, American Mathematical Society, 2022.

[14] R. A. Fisher, *The wave of advance of advantageous genes*, Annals of Eugenics, 7 (1937), pp. 355–369.

[15] R. N. Gantner, L. Herrmann, and C. Schwab, *Quasi–Monte Carlo Integration for Affine-Parametric, Elliptic PDEs: Local Supports and Product Weights*, SIAM J. Numer. Anal., 56 (2018), pp. 111–135.

[16] D. Gilbarg and N. S. Trudinger, *Elliptic Partial Differential Equations of Second Order*, vol. 224, Springer, 1977.

[17] A. D. Gilbert, I. G. Graham, F. Y. Kuo, I. H. Sloan, and R. Scheichl, *Analysis of quasi-Monte Carlo methods for elliptic eigenvalue problems with stochastic coefficients*, Numer. Math., 142 (2019), pp. 863–915.

[18] I. G. Graham, F. Y. Kuo, J. A. Nichols, R. Scheichl, C. Schwab, and I. H. Sloan, *Quasi-Monte Carlo finite element methods for elliptic PDEs with lognormal random coefficients*, Numer. Math., 131 (2015), pp. 329–368.

[19] I. G. Graham, F. Y. Kuo, D. Nuyens, R. Scheichl, and I. H. Sloan, *Circulant embedding with QMC: analysis for elliptic PDE with lognormal coefficients*, Numer. Math., 140 (2018), pp. 479–511.

[20] P. A. Guth, V. Kaarnioja, F. Y. Kuo, C. Schillings, and I. H. Sloan, *A quasi-Monte Carlo method for optimal control under uncertainty*, SIAM/ASA J. Uncertain. Quantif., 9 (2021), pp. 354–383.

[21] P. A. Guth, V. Kaarnioja, F. Y. Kuo, C. Schillings, and I. H. Sloan, *Parabolic PDE-constrained optimal control under uncertainty with entropic risk measure using quasi-Monte Carlo integration*, Numer. Math., 156 (2024), pp. 565–608.

[22] H. Hakula, H. Harbrecht, V. Kaarnioja, F. Y. Kuo, and I. H. Sloan, *Uncertainty quantification for random domains using periodic random variables*, Numer. Math., 156 (2024), pp. 273–317.

[23] H. Harbrecht, M. Schmidlin, and C. Schwab, *The Gevrey class implicit mapping theorem with application to UQ of semilinear elliptic PDEs*, Math. Models Methods Appl. Sci., 34 (2024), pp. 881–917.

[24] Y. He and C. Schwab, *Analytic regularity and solution approximation for a semilinear elliptic partial differential equation in a polygon*, Calcolo, 61 (2024), p. 11.

[25] D. A. Hormuth, K. A. Al Feghali, A. M. Elliott, T. E. Yankeelov, and C. Chung, *Image-based personalization of computational models for predicting response of high-grade glioma to chemoradiation*, Scientific Reports, 11 (2021), p. 8520.

[26] D. A. Hormuth II, J. A. Weis, S. L. Barnes, M. I. Miga, E. C. Rericha, V. Quaranta, and T. E. Yankeelov, *Predicting in vivo glioma growth with the reaction diffusion equation constrained by quantitative magnetic resonance imaging data*, Physical Biology, 12 (2015), p. 046006.

[27] A. M. Jarrett, A. S. Kazerouni, C. Wu, J. Virostko, A. G. Sorace, J. C. DiCarlo, D. A. Hormuth, D. A. Ekrut, D. Patt, B. Goodgame, S. Avery, and T. E. Yankeelov, *Quantitative magnetic resonance imaging and tumor forecasting of breast cancer patients in the community setting*, Nature Protocols, 16 (2021), pp. 5309–5338.

[28] A. Kolmogoroff, I. Petrovsky, and N. Piscounoff, *Study of the diffusion equation with growth of the quantity of matter and its application to a biology problem*, in Dynamics of Curved Fronts, Elsevier, 1988, pp. 105–130.

[29] F. Y. Kuo, C. Schwab, and I. H. Sloan, *Quasi-Monte Carlo finite element methods for a class of elliptic partial differential equations with random coefficients*, SIAM J. Numer. Anal., 50 (2012), pp. 3351–3374.

[30] B. Liang, J. Tan, L. Lozenski, D. A. Hormuth, T. E. Yankeelov, U. Villa, and D. Faghihi, *Bayesian inference of tissue heterogeneity for individualized prediction of glioma growth*, IEEE Trans. Med. Imaging, 42 (2023), pp. 2865–2875.

[31] F. Lindgren, H. Rue, and J. Lindström, *An explicit link between Gaussian fields and Gaussian Markov random fields: the stochastic partial differential equation approach*, J. R. Stat. Soc. Ser. B. Stat. Methodol., 73 (2011), pp. 423–498.

[32] M. Loève, *Probability Theory II*, vol. 46 of Graduate Texts in Mathematics, Springer, New York, 4 ed., 1978.

[33] G. Lorenzo, T. J. Hughes, P. Dominguez-Frojan, A. Reali, and H. Gomez, *Computer simulations suggest that prostate enlargement due to benign prostatic hyperplasia mechanically impedes prostate cancer growth*, Proc. Nat. Acad. Sci., 116 (2019), pp. 1152–1161.

[34] K.-A. Mardal, M. E. Rognes, T. B. Thompson, and L. M. Valnes, *Mathematical Modeling of the Human Brain: From Magnetic Resonance Images to Finite Element Simulation*, vol. 10, Springer Nature, 2022.

[35] S. J. McMahon, *The linear quadratic model: usage, interpretation and challenges*, Physics in Medicine & Biology, 64 (2018), p. 01TR01.

[36] J. D. Murray, *Mathematical Biology II: Spatial Models and Biomedical Applications*, vol. 18, Springer Science & Business Media, 2003.

[37] V. K. Nguyen, *Analyticity of parametric elliptic eigenvalue problems and applications to quasi-Monte Carlo methods*, Complex Var. Elliptic Equ., 69 (2024), pp. 1–21.

[38] G. Pash, U. Villa, D. A. Hormuth II, T. E. Yankeelov, and K. Willcox, *Predictive digital twins with quantified uncertainty for patient-specific decision making in oncology*, arXiv preprint arXiv:2505.08927, (2025).

[39] B. Perthame, *Parabolic Equations in Biology*, Springer, 2015.

[40] R. Rockne, E. Alvord Jr, J. K. Rockhill, and K. R. Swanson, *A mathematical model for brain tumor response to radiation therapy*, J. Math. Biol., 58 (2009), pp. 561–578.

[41] D. Stanzione, J. West, R. T. Evans, T. Minyard, O. Ghattas, and D. K. Panda, *Frontera: The Evolution of Leadership Computing at the National Science Foundation*, in Practice and Experience in Advanced Research Computing 2020: Catch the Wave, New York, NY, USA, 2020, Association for Computing Machinery, p. 106–111.

[42] A. M. Stuart, *Inverse problems: A Bayesian perspective*, Acta Numer., 19 (2010), pp. 451–559.

[43] R. Stupp, W. P. Mason, M. J. Van Den Bent, M. Weller, B. Fisher, M. J. Taphoorn, K. Belanger, A. A. Brandes, C. Marosi, U. Bogdahn, et al., *Radiotherapy plus concomitant and adjuvant temozolomide for glioblastoma*, New England Journal of Medicine, 352 (2005), pp. 987–996.

[44] K. R. Swanson, E. C. Alvord Jr, and J. D. Murray, *A quantitative model for differential motility of gliomas in grey and white matter*, Cell Proliferation, 33 (2000), pp. 317–329.

[45] F. Tröltzsch, *Optimal Control of Partial Differential Equations: Theory, Methods, and Applications*, vol. 112, American Mathematical Society, 2010.

[46] U. Villa and T. O'Leary-Roseberry, *A note on the relationship between PDE-based precision operators and Matérn covariances*, arXiv preprint arXiv:2407.00471, (2024).

[47] U. Villa, N. Petra, and O. Ghattas, *HIPPYlib: an extensible software framework for large-scale inverse problems governed by PDEs: Part I: deterministic inversion and linearized Bayesian inference*, ACM Trans. Math. Software, 47 (2021), pp. 1–34.